

# The chromatin modifier *Satb1* regulates cell fate through Fgf signalling in the early mouse embryo

Mubeen Goolam<sup>1</sup> and Magdalena Zernicka-Goetz<sup>1,\*</sup>

<sup>1</sup> University of Cambridge, Department of Physiology, Development & Neuroscience; Downing Street, Cambridge, CB2 3EG, UK

\*corresponding author: mz205@cam.ac.uk

**Key words:** *Satb1*, Epiblast, Primitive endoderm, Cell lineage specification, Preimplantation, Mouse

**Summary statement:** We identify a novel role for *Satb1* in regulating the cell fate choice between pluripotency and differentiation in the early mouse embryo.

## Abstract

The separation of embryonic from extra-embryonic tissues within the inner-cell-mass (ICM) to generate the epiblast (EPI), that will form the new organism, from the primitive endoderm (PE), that will form the yolk sac, is a crucial developmental decision. Here we identify a chromatin modifier, *Satb1*, with a distinct role in this decision. *Satb1* is differentially expressed within 16-cell-stage embryos with higher expression levels in the ICM progenitor cells. Depleting *Satb1* increases the number of EPI cells at the expense of PE. This phenotype can be rescued by simultaneous depletion of both *Satb1* and *Satb2*, due to their antagonistic effect on the pluripotency regulator *Nanog*. Consequently, increasing *Satb1* expression leads to differentiation into PE and a decrease in EPI, due to the modulation of expression of several pluripotency- and differentiation-related genes by *Satb1*. Finally, we show that *Satb1* is a downstream target of the Fgf signalling pathway, linking chromatin modification and Fgf signalling. Together, these results identify a role for *Satb1* in the lineage choice between pluripotency and differentiation and further our understanding of early embryonic lineage segregation.

## Introduction

The early mammalian embryo must correctly specify three distinct cell lineages: the epiblast (EPI), which gives rise to the embryo proper, and the two extraembryonic lineages, the trophectoderm (TE) and the primitive endoderm (PE), which go on to form critical supportive structures, the placenta and the yolk sac. By the 16-cell stage, the mouse embryo has a population of outside and inside cells that follow different fates. The outside cells will give rise to the TE whereas inside cells will form the pluripotent inner cell mass (ICM) of the blastocyst. The PE and the EPI are both derived from the ICM of the early blastocyst. Previous research has shown that in the early blastocyst the ICM contains a mixed population of PE and EPI progenitors in a mosaic 'salt and pepper' distribution which sort themselves into distinct layers by the time the blastocyst is ready to implant (E4.5) through active cell movements (Chazaud et al., 2006; Kurimoto et al., 2006; Meilhac et al., 2009; Plusa et al., 2008). Even though they are a mixed population early on, the individual cells in the early blastocyst are distinct enough that they go on to form either PE or EPI, but rarely both (Morris et al., 2010). It was shown that EPI precursors, expressing the pluripotency marker *Nanog*, secrete *Fgf4* ligand in the ICM which can initiate a signalling cascade in *Gata6* positive PE precursors that have the *Fgfr2* receptor highly expressed on their membranes (Frankenberg et al., 2011; Kurimoto et al., 2006; Morris et al., 2013; Ohnishi et al., 2014). This *Fgf* signalling is crucial for preventing *Nanog* from inhibiting *Gata6* and committing cells to a PE cell fate (Frankenberg et al., 2011; Kang et al., 2013; Krawchuk et al., 2013; Schrode et al., 2014). Indeed, when *Fgf* signalling is inhibited, all ICM cells are directed towards a *Nanog* positive EPI cell fate without forming any PE, while over expression results in the opposite phenotype, with all cells being converted into *Gata6* and *Sox17* positive PE (Chazaud et al., 2006; Feldman et al., 1995; Frankenberg et al., 2011; Nichols et al., 2009; Yamanaka et al., 2010). While the role of *Fgf* signalling has been well described in the embryo, much still remains unknown about how the cell fate choice between PE and EPI occurs. Our aim was to contribute to the identification of novel regulators of this lineage decision process.

When we mined a pre-existing dataset for genes differentially expressed between the first precursors of ICM (inside cells) and TE (outside cells) at the 16-cell stage (Graham et al., 2014), our attention was drawn to *Satb1*, a chromatin modifier, which was three times more highly expressed in inside cells compared to outside cells, potentially indicating a role within the ICM. Although the role of *Satb1* in the early mouse embryo is unknown, it has been shown to regulate pluripotency in mouse embryonic stem cells (Savarese et al., 2009), self-renewal

and pluripotency in both hematopoietic (Will et al., 2013) and trophoblast (Asanoma et al., 2012) stem cells and to promote the differentiation of hematopoietic stem cells (Satoh et al., 2013). Here, we wished to test the hypothesis that *Satb1* contributes to lineage specification within the early mouse embryo.

## Results

### Temporal and spatial expression of *Satb1* in preimplantation development

To investigate the potential role of *Satb1* in early mouse embryos, we first used qRT-PCR to analyse its expression throughout preimplantation development. This revealed high levels of maternal *Satb1* mRNA at the zygote and two-cell stages, before the zygotic genome is activated, a drop in *Satb1* at the four-cell stage before expression increased at 8-cell and was fairly stable until the blastocyst stage (Fig. 1 A). The presence of maternal mRNA and the stable levels of expression after the 8-cell stage prompted us to investigate *Satb1* protein levels by immunofluorescence. We found that the overall expression of protein was highly similar to that of the mRNA with maternal protein present in the zygote and at the two-cell stage and a drop in expression by the four-cell stage (Fig. 1 B, C). Protein levels increased at the 8-cell (in a relatively homogenous fashion; Fig. S1 A, B) and 16-cell stages with *Satb1* protein still present until the blastocyst stage in both the TE and ICM (Fig. 1 B, C).

We first identified *Satb1* as a gene of interest when examining our earlier mRNA sequencing results (Graham et al., 2014) that revealed it to be three times more highly expressed in inside cells compared to outside cells at the 16-cell stage. To confirm this expression pattern, we determined *Satb1* mRNA levels in inside and outside cells using qRT-PCR. To isolate the individual populations of inside or outside cells, we labelled 16-cell stage embryos by briefly incubating them in a suspension of 0.2µm fluorescent beads and then segregating inside and outside cells by gentle pipetting, as has been done previously (Graham et al., 2014). Separated individual outside (fluorescent) and inside (non-fluorescent) cells were pooled together for mRNA extraction (Fig. 1 D). In total, 35 inside cells and 41 outside cells (over three experiments) were collected. Inside cells were found to have over 3.5 times more *Satb1* mRNA than outside cells (Fig. 1 E,  $p < 0.001$ ).

Since *Satb1* protein expression peaked at the 16-cell stage, we next investigated if the differential expression of *Satb1* mRNA at the 16-cell stage is recapitulated on a protein level. Fluorescence intensity measurements of *Satb1* staining for outside cells (those that had at

least one domain in contact with the outside of the embryo) were compared to the intensity of inside cells (cells that were entirely surrounded by other cells) relative to DAPI. Intensity measurements were done on the layer-normalised sections using the IMAGEJ measure function. We found that inside cells had over 2x more Satb1 protein than the outside cells (Fig. 1 F, G). These results indicate that on both a protein and mRNA level Satb1 is differentially expressed at the 16-cell stage.

### **Depletion of Satb1 increases number of pluripotent cells**

To determine whether Satb1 might play any role in the preimplantation embryo, we next decreased its expression using a combination of three Satb1 specific siRNAs. We first confirmed that these siRNAs reduced Satb1 levels on both mRNA and protein levels despite the prevalence of maternal protein and mRNA (Fig. 2 A, B) and that the reduction in Satb1 protein persisted until the blastocyst stage (Fig. S1 C, D). To test the effect of Satb1 knockdown, we injected zygotes with Satb1 siRNA and cultured embryos until the blastocyst stage to compare the cell lineage allocation to embryos injected with a control siRNA (Fig. 2 C). We found that Satb1 RNAi blastocysts had a severely reduced number of PE cells as assessed by Sox17 expression (Fig. 2 D, E, Fig. S2). The total number of cells (average of 105 in control and 103 in Satb1 siRNA) as well as the number of TE cells (Cdx2 positive cells - average of 86 in control and 83 in Satb1 siRNA) did not change after Satb1 RNAi (Fig. 2 D, E). Importantly, we found that, the 38% reduction in PE cells was met with a 47% increase in EPI cells as assessed by the expression of Nanog and Sox17 (Fig. 2 D, E), suggesting that reduced levels of Satb1 biases the ICM to produce more EPI rather than PE. To confirm this result, we next injected each Satb1 siRNA individually. We observed the same developmental defect using individual siRNAs as noted with the combination of Satb1 siRNAs with a reduction in PE cells and an increase in EPI cells (Fig. S1 E, F). This phenotype was further found to be proportional to the efficacy of Satb1 knockdown (Fig. S1 G), indicating that the bias in cell fate observed upon Satb1 depletion is specific to decreased Satb1 and not due to off-target effects. We further validated these findings by assessing the expression of two additional PE markers, Gata6 and Pdgfra, as well as an additional EPI marker, Sox2, after Satb1 RNAi, and found a similar bias with Satb1 reduced embryos having an increase in EPI and a decrease in PE by the blastocyst (Fig. S3). We next investigated the timing of the effect of Satb1 RNAi in the embryo. We found that at the 16-cell stage (Fig. S4. A, B) and at the initiation of the blastocyst, the 32-cell stage, (Fig. S4 C, D) there was no effect on the distribution or expression pattern of Gata6 or Nanog after Satb1 RNAi. However, by the early

blastocyst stage we noted a significant reduction in the number of cells expressing Gata6 after Satb1 RNAi (Fig. S4 E, F). These data suggest that while Satb1 has no effect on the initiation of PE specification it does have a specific role in PE lineage commitment.

The reduction in PE and increase in EPI after Satb1 RNAi suggested that it could have a role in the cell fate choice within the ICM. To verify this result, we next determined if individual blastomeres with reduced Satb1 could have preferential fate. To this end, we injected one blastomere of two-cell stage embryos with Satb1 or control siRNA, together with the membrane bound phosphoprotein Gap43-GFP (Benowitz and Routtenberg, 1987) mRNA which can serve as a marker of cell lineage by labelling the membranes of injected cells (Fig. 2 F). The embryos were cultured for 72 hours, until the late blastocyst stage, and the contribution to TE, EPI and PE was scored by assessing molecular markers for each lineage and cell position within the embryo. In comparison to control injected embryos, we found that Satb1 siRNA injected blastomeres contributed significantly more to the EPI (Fig. 2 G, H;  $p < 0.001$ ). Consequently, Satb1 siRNA injected blastomeres also contributed significantly fewer cells to the PE (Fig. 2 G, H;  $p < 0.001$ ; cells contributed to the PE: 4.96 in control embryos, 2.28 in Satb1 RNAi embryos). In agreement with previous results, injection of Satb1 siRNA into half of the embryo had no effect on relative total contribution of injected cells, or the contribution to the TE when compared to control injected embryos (Fig. 2 G, H). These results indicate that clonal depletion of Satb1 biases cell fate choice in the embryo: cells with lower Satb1 will preferentially give rise the EPI as opposed to the PE.

### **Increasing Satb1 decreases the number of pluripotent cells**

Since reducing Satb1 directs cells towards the pluripotent lineage, we hypothesised that Satb1 might have a role in promoting a PE lineage. To investigate Satb1's expression pattern in presumptive PE and EPI cells, we analysed Satb1 expression, together with Gata6 (a marker of PE progenitors), in the blastocyst ICM. We found Satb1 expression was significantly higher in PE precursors as opposed to EPI precursors (Fig. 3 A, B;  $p < 0.001$ ) as would be expected of a gene with a role in PE specification. To investigate if overexpressing Satb1 might have the opposite effect to its reduction, we reverse transcribed mRNA from a Satb1 cDNA, injected it into zygotes (400ng/ $\mu$ l) and let embryos develop until morula stage when we analysed them by qRT-PCR. We found that the injection of Satb1 mRNA resulted in a more than 2-fold increase in Satb1 mRNA levels (Fig. 3 C;  $p < 0.05$ ), indicating overexpressing Satb1 is effective. To test whether overexpressing Satb1 mRNA was able to

rescue the phenotype seen after Satb1 siRNA we depleted Satb1 siRNA in the zygote and then overexpressed Satb1 mRNA in both blastomeres of the two-cell stage embryo (Fig. S5 A). Overexpression of Satb1 was able to return the number PE and EPI cells to similar levels as to controls, providing evidence for the specificity of the siRNA phenotype (Fig. S5 B, C).

To test the consequences of increasing Satb1 mRNA on lineage allocation, we first injected Satb1 mRNA into zygotes and allowed them to develop until the blastocyst stage and compared the contribution of mRNA injected embryos to TE, EPI and PE (Fig. 3 D). Overexpression of Satb1 resulted in a significant increase in the number of PE cells ( $p < 0.01$ ) and a significant decrease in the number of EPI cells ( $p < 0.01$ ) when compared to controls (Fig. 3 E, F), the opposite effect of what we found when knocking down Satb1. These results indicate that modulating the levels of Satb1 has a specific effect on the differentiation of the ICM into PE or EPI: an increase in Satb1 levels pushes ICM cells to preferentially form PE instead of EPI.

To further verify this result, we also determined the lineage contribution when increasing Satb1 clonally. To this end, we injected 400ng/ $\mu$ l of Satb1 mRNA together with Gap43-GFP mRNA into one blastomere of a two-cell embryo, cultured the embryos to the blastocyst stage and assessed lineage contribution using molecular markers as well as cell position (Fig. 3 G). We found that Satb1 mRNA injection resulted in a significant decrease in contribution to the EPI (Fig. 3 H, I;  $p < 0.05$ ; cells contributed to the EPI: 5.16 in control embryos, 3.61 in Satb1 RNAi embryos) as well as a significant increase in PE contribution relative to control (Fig. 3 H, I). These results were not due to a reduction in total or TE cell contributions as both Satb1 mRNA and control mRNA embryos were similar in their TE and total cell number (Fig. 3 H, I). Therefore, clonal overexpression of Satb1 biases ICM cells to form PE and not EPI. Collectively, these results, together with the clonal siRNA results, indicate that modulating the amount of Satb1 in the embryo has a specific effect on cell fate choice within the ICM.

### **Simultaneous depletion of Satb1 and Satb2 rescues Satb1 depletion**

Satb2 is closely related to Satb1 and it has been shown that knocking down both Satb1 and Satb2 simultaneously in mESCs can rescue the impaired differentiation noted in Satb1<sup>-/-</sup> mESCs (Savarese et al., 2009). We therefore decided to investigate if Satb2 RNAi could also rescue the Satb1 siRNA phenotype in the embryo. We first tested the effectiveness of Satb2



siRNA using qRT-PCR. To this end, Satb1 siRNA, Satb2 siRNA or a combination of both was injected into zygotes at a final total concentration of 12 $\mu$ M and embryos were collected at the 16-cell stage for mRNA extraction. We found that the knockdown of Satb2 siRNA did not affect Satb1 mRNA levels but was effective in reducing Satb2 mRNA by 63% when compared to control (Fig. 4 A;  $p < 0.01$ ). Interestingly, Satb1 RNAi resulted in a more than 2-fold increase in Satb2 mRNA while reducing Satb1 mRNA by almost 70% (Fig. 4 A;  $p < 0.001$ ). The opposite result was found when Satb1 was overexpressed with a 50% reduction in Satb2 mRNA along with a 2-fold increase in Satb1 mRNA (Fig. S6;  $p < 0.05$ ). These results show that RNAi for both of these closely related genes is specific to each gene and that Satb1 might be a negative regulator of Satb2. Additionally, double knockdown of Satb1 and Satb2 reduced the levels of both mRNAs to about 40% of the controls (Fig. 4 A;  $p < 0.01$ ), indicating that the siRNAs can work simultaneously without interfering with one another when injected into the same embryos.

We next determined the effect of Satb2 siRNA on lineage specification and whether or not it could rescue the Satb1 siRNA phenotype. To this end, Satb1 siRNA, Satb2 siRNA or a combination of both were injected into zygotes at a final total concentration of 12 $\mu$ M and embryos were allowed to develop until E4.5 when their lineage specification was evaluated (Fig. 4 B). We found that Satb2 siRNA by itself had no effect on preimplantation development with a similar number of TE, PE and EPI cells present compared to controls (Fig. 4 C, D). However, double knockdown of Satb1 and Satb2 siRNA was able to significantly rescue the Satb1 siRNA phenotype leading to the number of EPI and PE cells being more similar to controls (Fig. 4 C, D). These results indicate that Satb2 and Satb1 have antagonistic effects on cell fate choice within the ICM.

### **Satb1 modulates the expression of cell fate regulators**

Since our results indicate that modulating the levels of Satb1, and to a lesser degree Satb2, effects the cell fate choice within the ICM, we next wished to determine the changes in gene expression as a result of changing the levels of Satb1 and Satb2, concentrating on key cell fate determinants at this stage. To this end, we injected Satb1 siRNA, or Satb1 mRNA, or Satb2 siRNA, or Satb2 mRNA into zygotes and allowed them to develop until the morula stage (about the 32-cell stage) before mRNA extraction (Fig. 5 A, A'). We found that Satb1 RNAi resulted in a significant increase in key EPI regulators Nanog, Oct4 and Sox2 (Fig. 5 A; 3.9-fold, 2.5-fold and 1.98-fold respectively,  $p < 0.001$ ,  $p < 0.01$ ). It also resulted in a



significant decrease in the differentiation markers of the TE such as *Cdx2* ( $p < 0.05$ ) and *Id2* ( $p < 0.001$ ) and also PE marker genes such as *Gata6* ( $p < 0.01$ ) and *Sox17* ( $p < 0.01$ ). As expected, injection of *Satb1* mRNA had the opposite effect, with a decrease in *Nanog* and increases in *Id2*, *Gata6* and *Sox17* expression (Fig. 5 A;  $p < 0.05$  and  $p < 0.001$ ). *Satb2* RNAi also resulted in decreased expression of *Nanog* (Fig. 5 A';  $p < 0.05$ ) but did not alter the expression of any of the other genes examined here (Fig. 5 A'), perhaps accounting for the lack of a phenotype noted after *Satb2* RNAi. Interestingly, overexpression of *Satb2* resulted in an almost 2-fold increase in *Nanog*, *Oct4* and *Sox2* without affecting the other lineage markers (Fig. 5 A';  $p < 0.05$ ,  $p < 0.01$ ) indicating a potential role in promoting an EPI lineage. In agreement with this, we found *Satb2* to be co-expressed with *Nanog* in the early blastocyst and consequently to be significantly more highly expressed in EPI cells as opposed to PE cells by the late blastocyst (Fig. S7 A, A', B;  $p < 0.001$ ). Overall, these results indicate that *Satb1* modulates the expression of cell fate regulators during preimplantation development and that *Satb1* and *Satb2* have antagonistic effects on *Nanog* expression within the early embryo.

### **Fgf signalling regulates *Satb1***

Since the above results indicated that *Satb1* is involved in the specification of PE and EPI in the ICM, we next wished to determine the upstream regulator of *Satb1*. It has been shown that the inhibition of Fgf signalling influenced mESCs dependence on *Satb1* (Savarese et al., 2009). This is particularly interesting as Fgf signalling is crucial to PE fate specification (Frankenberg et al., 2011; Kang et al., 2013; Morris et al., 2013; Yamanaka et al., 2010). To determine whether inhibition of the Fgf signalling pathway affects *Satb1* expression in the early mouse embryo, we determined the effects of two different Fgf signalling pathway inhibitors on *Satb1* expression. We used an Fgf receptor inhibitor (Morris et al., 2013; Nichols et al., 2009; Yamanaka et al., 2010) and a Mek inhibitor (Nichols et al., 2009; Schrode et al., 2014; Yamanaka et al., 2010) as they are well documented to block PE formation in the embryo. We treated two-cell stage embryos with the Fgf receptor inhibitor at a concentration of 100nM (Morris et al., 2012) and the Mek inhibitor at a concentration of 0.5 $\mu$ M (Yamanaka et al., 2010) and then let the embryos develop until the 8-cell stage when they were fixed and immunostained for *Satb1* (Fig. 6 A). We found that embryos treated with either inhibitor showed a significant decrease in *Satb1* protein by the 8-cell stage (Fig. 6 B, C  $p < 0.001$ ).

To examine if the reduction in Satb1 levels after Fgf inhibition could be rescued by the addition of exogenous Satb1 mRNA we injected Satb1 mRNA into embryos at the 2-cell stage and then treated them with inhibitors until the 8-cell stage (Fig. 6 A). In these embryos, Satb1 was returned to similar levels as in controls (Fig. 6 B, D). These results suggest that Fgf signalling is involved in the regulation of Satb1 in the preimplantation mouse embryo.

## Discussion

The specification of three distinct cell lineages in the mouse embryo occurs during two cell fate decisions. The first cell fate decision physically separates the population of ICM and TE cells while the second cell fate decision further specifies the ICM into the PE and the EPI. It is critical that all three lineages are correctly specified in order to form a blastocyst capable of implanting into the uterine wall and developing further. Here, aiming to identify novel regulators that control cell fate choice in preimplantation development, we discovered the chromatin modifier Satb1 as an important player. Satb1 was first identified in thymocytes where it is known to regulate gene expression by organising the structure of higher-order chromatin into loop domains and by acting as a 'landing platform' for chromatin remodelling enzymes (Cai et al., 2006; Yasui et al., 2002). In mESCs, Satb1 was shown to regulate pluripotency by directly repressing Nanog: Satb1 knock out mESCs maintained Nanog expression even when placed into differentiation medium (Savarese et al., 2009). However, the role of Satb1 in the preimplantation embryo remains unknown. Here we find that expression of Satb1 protein is specifically upregulated, on both mRNA and protein levels, in the inner cells of 16-cell stage embryos when the ICM is first specified, indicating a potential role within the specification of these cells. We further find that Satb1 is specifically upregulated within the PE precursors signifying its potential importance to the specification of the PE. We confirm this hypothesis by downregulating Satb1 which we show leads to a reduction in the number of PE cells and an increase in the number of EPI cells by the blastocyst stage. In agreement with this, overexpression of Satb1 has an opposite effect on lineage specification and promotes a PE lineage within the ICM. Our clonal knockdown and overexpression experiments further support these findings as we find that blastomeres with reduced Satb1 preferentially gave rise to EPI and those with increased Satb1 preferentially gave rise to PE. We find that Satb1 does not have an effect on the 16-32 cell stage embryo when PE specification is initiated. Rather it has a role in the commitment of cells within the blastocyst to the PE lineage. We further find that this change in cell fate is due to modulating the expression of a series of lineage specific genes downstream of Fgf signalling.

We find that while modulating *Satb1* expression clearly effects cell fate commitment in the preimplantation mouse embryo, it rarely resulted in a complete ablation of either the PE or EPI lineages. This is important when viewed in context of the *Satb1* knockout mice which survive during embryogenesis, although die by three weeks of age (Alvarez et al., 2000). If *Satb1* is important for the regulation of a balance between pluripotency/differentiation as has been shown here, how can this be reconciled with the lack of a preimplantation phenotype in knockout mice? It has previously been shown that the minimum requirement for successful development is 3-4 pluripotent cells by the time of implantation (Morris et al., 2012; Soriano and Jaenisch, 1986). If *Satb1*<sup>-/-</sup> embryos did have a phenotype, based on the results from this study, they would most likely have an ICM with high numbers of EPI cells and a low number of PE cells. Similar phenotypes have been found in *Fgf4*<sup>+/-</sup> and *Gata6*<sup>+/-</sup> embryos and in both cases embryos were able to recover by E4.5 (Bessonard et al., 2014; Krawchuk et al., 2013). Therefore, it is possible that while *Satb1* helps to organise and specify the correct number of PE and EPI cells within the ICM, it might not be absolutely essential for embryo survival and can be compensated for, in agreement with the highly regulative nature of mammalian development.

*Satb1* is closely related to another family member, *Satb2*, leading us to investigate if *Satb2* might also have a function in preimplantation development. We find that while down-regulating *Satb2* by itself has no effect on development, depletion of both genes at once, is able to partially rescue the *Satb1* RNAi phenotype. This is in agreement with the results in mESCs, as knockdown of both *Satb1* and *Satb2* rescued the disruption in differentiation noted in *Satb1*<sup>-/-</sup> mESCs (Savarese et al., 2009). Our results indicate that this is likely because knocking down *Satb2* reduces *Nanog* mRNA, the opposite effect to reducing *Satb1*. In agreement with this, overexpression of *Satb2* is able to increase *Nanog* expression providing evidence that *Satb2* is a positive regulator of *Nanog*. *Satb1* and *Satb2* therefore have antagonistic effects on *Nanog* expression. Thus, we hypothesise that when just *Satb1* is reduced it releases its repression on both *Nanog* and *Satb2* and this is enough to bias cell fate choice towards the EPI. This bias is strengthened by the fact that *Satb1* also acts as a positive regulator of PE differentiation factors *Sox17* and *Gata6*. Knocking down both *Satb1* and *Satb2* removes both the repression and activation of *Nanog* expression with the net effect of normalising *Nanog* expression levels. The results we present here showing the effect of *Satb2* on *Nanog* might help to explain why it has been impossible to derive *Satb2*<sup>-/-</sup> mESCs

(Savarese et al., 2009) as without appropriate expression level of Nanog, it would be impossible to derive functional ESC clones.

The effect of Satb2 on Nanog expression raises the question of why reducing Satb2 levels in the embryo did not affect development to the same degree as modulation of Satb1. One explanation is that while Satb2 siRNA was able to reduce Nanog levels, more than 65% of Nanog mRNA was still present after RNAi. While Nanog is a crucial factor in determining cell fate, in the highly regulative mouse embryo a 35% reduction in Nanog levels may not be sufficient to drive cell fate changes. Additionally, our results suggest that while Satb2 might affect just Nanog expression in embryos, Satb1 has effects on the expression of multiple genes including *Cdx2*, *Gata6*, *Id2* and *Sox17*. The same pattern, albeit with the opposite effects on expression, was noted for overexpression of Satb1 and Satb2. The combined effects of Satb1, on numerous genes, are sufficient to drive cell fate changes within the ICM. Modulating Satb2 however, only moderately affects Nanog. This can also explain why the double knockdown of Satb1 and Satb2 only results in a partial rescue of the Satb1 siRNA phenotype, because while Nanog expression levels might be saved, the effects on the other genes regulated by Satb1 are not.

Finally, our results indicate that Satb1 expression is controlled by Fgf signalling as we find that inhibition of Fgf signalling, inhibits Satb1 expression, which can be restored by the addition of exogenous Satb1 mRNA. We also attempted to rescue the perturbation in cell fate that is noted after Fgf signalling inhibition (Nichols et al., 2009; Schrode et al., 2014; Yamanaka et al., 2010) by overexpressing Satb1 mRNA but were unable to restore the expression of PE markers by the blastocyst stage (data not shown). We predict this is because the Fgf signalling pathway has a wide variety of targets in the mouse embryo, and so rescuing one downstream pathway is not sufficient to overcome the multiple effects of inhibiting Fgf signalling. In agreement, repression of Fgf signalling results in a similar but much stronger phenotype compared to down-regulation of Satb1, with all ICM cells expressing EPI lineage markers (Frankenberg et al., 2011; Yamanaka et al., 2010). This indicates that Satb1 might be one of the links between Fgf signalling and its downstream targets in early mouse embryos. In agreement with this, Fgf signalling and Satb1 both promote stem cell maintenance and proliferation and inhibit differentiation of trophoblast stem cells (Asanoma et al., 2012; Tanaka et al., 1998).

Taken together, our results suggest that *Satb1* might act as a chromatin modifier modulating gene expression downstream of Fgf signalling pointing to a crucial missing step of chromatin remodelling that can serve to establish the progenitors of the two distinct lineages within the ICM. We speculate that *Satb1* could potentially act in two manners to direct ICM cell fate. Firstly, as *Satb1* has been found, through co-immunoprecipitation experiments, to directly bind to the 5' flanking sequence of *Nanog* in mESCs (Savarese et al., 2009), we predict that *Satb1* would also bind directly upstream of *Nanog* to repress its transcription in mouse embryos. Secondly, since we find that *Satb1* can regulate the expression of numerous genes in the mouse embryo, we predict that this is a function of its ability to act as a 'landing platform' that is able to recruit chromatin remodelling enzymes to activate or repress gene expression as has been shown previously (Yasui et al., 2002).

In conclusion, it can be hypothesised that cells within the ICM have different levels of Fgf receptor, *Fgfr2*, on their membranes, as has been previously shown (Guo et al., 2010; Krupa et al., 2014; Kurimoto et al., 2006; Morris et al., 2013; Ohnishi et al., 2014). Cells with more receptor are more susceptible to Fgf ligand (which is secreted by the inside cells at this stage) and thus have higher levels of *Satb1* (Fig. 7). Higher expression of *Satb1* would lead to the inhibition of the pluripotency factors *Nanog* and *Satb2* which in turn would lead them to initiate differentiation into the PE lineage (Fig. 7). Cells that are less susceptible to Fgf4 signalling will have reduced *Satb1* which, in turn, leads to more *Nanog* expression and therefore biases cell fate towards the pluripotent EPI lineage. Additionally, loss of both *Satb1* and *Satb2* removes both an activator and repressor of *Nanog* resulting in the formation of a normal ICM (Fig. 7). This hypothesis, based on the results we present here, helps to further our understanding of the mechanism that leads to resolution of the 'salt and pepper' distribution of *Gata6*- and *Nanog*-expressing progenitors within the ICM.

## **Materials and Methods**

### **Collection of mouse embryos**

Embryo recovery was done on superovulated F1 (C57Bl/6xCBA) females between 4-6 weeks old as has been described previously (Piotrowska et al., 2001) Following collection or experimental manipulation, embryos were cultured in drops of KSOM (Millipore) supplemented with 4mg/ml BSA under paraffin oil at 37.5°C in 5% CO<sub>2</sub>.

### **Collection of individual cells**

Individual cells for qRT-PCR were collected at the 16-cell stage (78 hrs after hCG) as has been done previously (Graham et al., 2014). Embryos were isolated directly at 16-cell and incubated in M2 with a fluorescently labelled 0.2 mm microsphere suspension (Polysciences, Inc.) diluted to 1:50 for 30 seconds. Outside (strongly fluorescent) and inside (non-fluorescent) cells were collected, grouped and placed into Arcturus Biosciences PicoPure RNA isolation kit extraction buffer for mRNA isolation.

### **Treatment with chemical inhibitors**

To inhibit Fgf signalling embryos were treated from the zygote to 8-cell stage with an Fgf receptor inhibitor at a concentration of 100nM (Stemgent; PD173074) or a Mek inhibitor (Stemgent; PD0325901) at a concentration of 0.5 $\mu$ M both in KSOM. Inhibitors were dissolved in DMSO (final concentration of DMSO was 0.005%). Control embryos were incubated in the equivalent DMSO concentration but in the absence of the inhibitor. Following treatment with inhibitors embryos were fixed and processed for immunostaining.

### **Microinjection of siRNAs and mRNAs**

All microinjections were done with siRNAs for *Satb1* and *Satb2* as well as AllStars Negative Control siRNA purchased from Qiagen. For siRNA sequences see Supplementary Materials and Methods. *Satb1* and *Satb2* cDNA (Dharmacon) was cloned into pRN3P as described previously (Zernicka-Goetz et al., 1997). *In vitro* transcription was undertaken on linearized cDNA using the mMessage mMachine T3 kit (Ambion) according to the manufacturer's instructions. Microinjection of embryos with siRNA (always at a final concentration of 12 $\mu$ M) or mRNA (together with Ruby mRNA (200ng/ $\mu$ l) or Gap43-GFP mRNA (400ng/ $\mu$ l) as markers of injection) was carried out in M2 covered in oil on a glass depression slide using a Femtojet micro-injection system (Eppendorf). Embryos were cultured in KSOM under paraffin oil at 37.5°C in a 5% CO<sub>2</sub>.

### **Immunofluorescence**

Immunofluorescence was carried out as described previously (Jedrusik et al., 2008). Multichannel Imaging was acquired on a Leica SP5 inverted confocal microscope using Leica LAS AF software and a 20x or 40x oil immersion objective. Confocal z-stacks were exported to IMAGEJ for image processing, intensity measurements and cell counting. For details of

immunofluorescence protocol and intensity measurements as well as antibody details see Supplementary Materials and Methods.

### **qRT-PCR**

qRT-PCR was carried out as has been done previously (Goolam et al., 2016). Gapdh or H2A.Z were used as endogenous controls. H2A.Z was used when different stages of preimplantation development were compared. Three biological repeats were undertaken for every qRT-PCR. For primer details see Supplementary Materials and Methods.

### **Statistical Analyses**

Unless otherwise specified Student's t-tests were used to test significance. \*=  $p < 0.05$  \*\*=  $p < 0.01$ , \*\*\*=  $p < 0.001$ . All error bars represent s.e.m.



## References

- Alvarez, J.D., Yasui, D.H., Niida, H., Joh, T., Loh, D.Y., and Kohwi-Shigematsu, T. (2000). The MAR-binding protein SATB1 orchestrates temporal and spatial expression of multiple genes during T-cell development. *Genes & development* *14*, 521-535.
- Asanoma, K., Kubota, K., Chakraborty, D., Renaud, S.J., Wake, N., Fukushima, K., Soares, M.J., and Rumi, M.A. (2012). SATB homeobox proteins regulate trophoblast stem cell renewal and differentiation. *The Journal of biological chemistry* *287*, 2257-2268.
- Benowitz, L.I., and Routtenberg, A. (1987). A membrane phosphoprotein associated with neural development, axonal regeneration, phospholipid metabolism, and synaptic plasticity. *Trends in Neuroscience* *10*, 527-532.
- Bessonard, S., De Mot, L., Gonze, D., Barriol, M., Dennis, C., Goldbeter, A., Dupont, G., and Chazaud, C. (2014). Gata6, Nanog and Erk signaling control cell fate in the inner cell mass through a tristable regulatory network. *Development (Cambridge, England)* *141*, 3637-3648.
- Cai, S., Lee, C.C., and Kohwi-Shigematsu, T. (2006). SATB1 packages densely looped, transcriptionally active chromatin for coordinated expression of cytokine genes. *Nature genetics* *38*, 1278-1288.
- Chazaud, C., Yamanaka, Y., Pawson, T., and Rossant, J. (2006). Early lineage segregation between epiblast and primitive endoderm in mouse blastocysts through the Grb2-MAPK pathway. *Developmental cell* *10*, 615-624.
- Feldman, B., Poueymirou, W., Papaioannou, V.E., DeChiara, T.M., and Goldfarb, M. (1995). Requirement of FGF-4 for postimplantation mouse development. *Science (New York, NY)* *267*, 246-249.
- Frankenberg, S., Gerbe, F., Bessonard, S., Belville, C., Pouchin, P., Bardot, O., and Chazaud, C. (2011). Primitive endoderm differentiates via a three-step mechanism involving Nanog and RTK signaling. *Developmental cell* *21*, 1005-1013.
- Goolam, M., Scialdone, A., Graham, S.J., Macaulay, I.C., Jedrusik, A., Hupalowska, A., Voet, T., Marioni, J.C., and Zernicka-Goetz, M. (2016). Heterogeneity in Oct4 and Sox2 Targets Biases Cell Fate in 4-Cell Mouse Embryos. *Cell* *165*, 61-74.
- Graham, S.J., Wicher, K.B., Jedrusik, A., Guo, G., Herath, W., Robson, P., and Zernicka-Goetz, M. (2014). BMP signalling regulates the pre-implantation development of extra-embryonic cell lineages in the mouse embryo. *Nature communications* *5*, 5667.
- Guo, G., Huss, M., Tong, G.Q., Wang, C., Li Sun, L., Clarke, N.D., and Robson, P. (2010). Resolution of cell fate decisions revealed by single-cell gene expression analysis from zygote to blastocyst. *Developmental cell* *18*, 675-685.
- Jedrusik, A., Parfitt, D.E., Guo, G., Skamagki, M., Grabarek, J.B., Johnson, M.H., Robson, P., and Zernicka-Goetz, M. (2008). Role of Cdx2 and cell polarity in cell allocation and specification of trophectoderm and inner cell mass in the mouse embryo. *Genes & development* *22*, 2692-2706.
- Kang, M., Piliszek, A., Artus, J., and Hadjantonakis, A.K. (2013). FGF4 is required for lineage restriction and salt-and-pepper distribution of primitive endoderm factors but not their initial expression in the mouse. *Development (Cambridge, England)* *140*, 267-279.
- Krawchuk, D., Honma-Yamanaka, N., Anani, S., and Yamanaka, Y. (2013). FGF4 is a limiting factor controlling the proportions of primitive endoderm and epiblast in the ICM of the mouse blastocyst. *Developmental biology* *384*, 65-71.
- Krupa, M., Mazur, E., Szczepanska, K., Filimonow, K., Maleszewski, M., and Suwinska, A. (2014). Allocation of inner cells to epiblast vs primitive endoderm in the mouse embryo is biased but not determined by the round of asymmetric divisions (8-->16- and 16-->32-cells). *Developmental biology* *385*, 136-148.

Kurimoto, K., Yabuta, Y., Ohinata, Y., Ono, Y., Uno, K.D., Yamada, R.G., Ueda, H.R., and Saitou, M. (2006). An improved single-cell cDNA amplification method for efficient high-density oligonucleotide microarray analysis. *Nucleic acids research* 34, e42.

Meilhac, S.M., Adams, R.J., Morris, S.A., Danckaert, A., Le Garrec, J.F., and Zernicka-Goetz, M. (2009). Active cell movements coupled to positional induction are involved in lineage segregation in the mouse blastocyst. *Developmental biology* 331, 210-221.

Morris, S.A., Graham, S.J., Jedrusik, A., and Zernicka-Goetz, M. (2013). The differential response to Fgf signalling in cells internalized at different times influences lineage segregation in preimplantation mouse embryos. *Open biology* 3, 130104.

Morris, S.A., Guo, Y., and Zernicka-Goetz, M. (2012). Developmental plasticity is bound by pluripotency and the Fgf and Wnt signaling pathways. *Cell reports* 2, 756-765.

Morris, S.A., Teo, R.T., Li, H., Robson, P., Glover, D.M., and Zernicka-Goetz, M. (2010). Origin and formation of the first two distinct cell types of the inner cell mass in the mouse embryo. *Proceedings of the National Academy of Sciences of the United States of America* 107, 6364-6369.

Nichols, J., Silva, J., Roode, M., and Smith, A. (2009). Suppression of Erk signalling promotes ground state pluripotency in the mouse embryo. *Development (Cambridge, England)* 136, 3215-3222.

Ohnishi, Y., Huber, W., Tsumura, A., Kang, M., Xenopoulos, P., Kurimoto, K., Oles, A.K., Arauzo-Bravo, M.J., Saitou, M., Hadjantonakis, A.K., *et al.* (2014). Cell-to-cell expression variability followed by signal reinforcement progressively segregates early mouse lineages. *Nature cell biology* 16, 27-37.

Piotrowska, K., Wianny, F., Pedersen, R.A., and Zernicka-Goetz, M. (2001). Blastomeres arising from the first cleavage division have distinguishable fates in normal mouse development. *Development (Cambridge, England)* 128, 3739-3748.

Plusa, B., Piliszek, A., Frankenberg, S., Artus, J., and Hadjantonakis, A.K. (2008). Distinct sequential cell behaviours direct primitive endoderm formation in the mouse blastocyst. *Development (Cambridge, England)* 135, 3081-3091.

Satoh, Y., Yokota, T., Sudo, T., Kondo, M., Lai, A., Kincade, P.W., Kouro, T., Iida, R., Kokame, K., Miyata, T., *et al.* (2013). The *Satb1* protein directs hematopoietic stem cell differentiation toward lymphoid lineages. *Immunity* 38, 1105-1115.

Savarese, F., Davila, A., Nechanitzky, R., De La Rosa-Velazquez, I., Pereira, C.F., Engelke, R., Takahashi, K., Jenuwein, T., Kohwi-Shigematsu, T., Fisher, A.G., *et al.* (2009). *Satb1* and *Satb2* regulate embryonic stem cell differentiation and *Nanog* expression. *Genes & development* 23, 2625-2638.

Schrode, N., Saiz, N., Di Talia, S., and Hadjantonakis, A.K. (2014). GATA6 levels modulate primitive endoderm cell fate choice and timing in the mouse blastocyst. *Developmental cell* 29, 454-467.

Soriano, P., and Jaenisch, R. (1986). Retroviruses as probes for mammalian development: allocation of cells to the somatic and germ cell lineages. *Cell* 46, 19-29.

Tanaka, S., Kunath, T., Hadjantonakis, A.K., Nagy, A., and Rossant, J. (1998). Promotion of trophoblast stem cell proliferation by FGF4. *Science (New York, NY)* 282, 2072-2075.

Will, B., Vogler, T.O., Bartholdy, B., Garrett-Bakelman, F., Mayer, J., Barreyro, L., Pandolfi, A., Todorova, T.I., Okoye-Okafor, U.C., Stanley, R.F., *et al.* (2013). *Satb1* regulates the self-renewal of hematopoietic stem cells by promoting quiescence and repressing differentiation commitment. *Nature immunology* 14, 437-445.

Yamanaka, Y., Lanner, F., and Rossant, J. (2010). FGF signal-dependent segregation of primitive endoderm and epiblast in the mouse blastocyst. *Development (Cambridge, England)* 137, 715-724.

Yasui, D., Miyano, M., Cai, S., Varga-Weisz, P., and Kohwi-Shigematsu, T. (2002). SATB1 targets chromatin remodelling to regulate genes over long distances. *Nature* 419, 641-645.  
Zernicka-Goetz, M., Pines, J., McLean Hunter, S., Dixon, J.P., Siemering, K.R., Haseloff, J., and Evans, M.J. (1997). Following cell fate in the living mouse embryo. *Development* (Cambridge, England) 124, 1133-1137.

### **Acknowledgments**

We are grateful to our colleagues for advice during this project and for help with critical reading of this manuscript. We thank Meng Zhu for assistance with graphical representations.

### **Author Contributions**

All experiments were performed by MG in MZG's laboratory. Data were analysed and interpreted by MG and MZG. The manuscript was written by MG and MZG.

### **Competing interests**

The authors declare no competing financial interests

### **Funding**

We are grateful to the Wellcome Trust Senior Research Fellowship to MZG who funded this work. The funders had no role in the design, experimentation, analysis of the experiments, or preparation of the manuscript.

# Figures

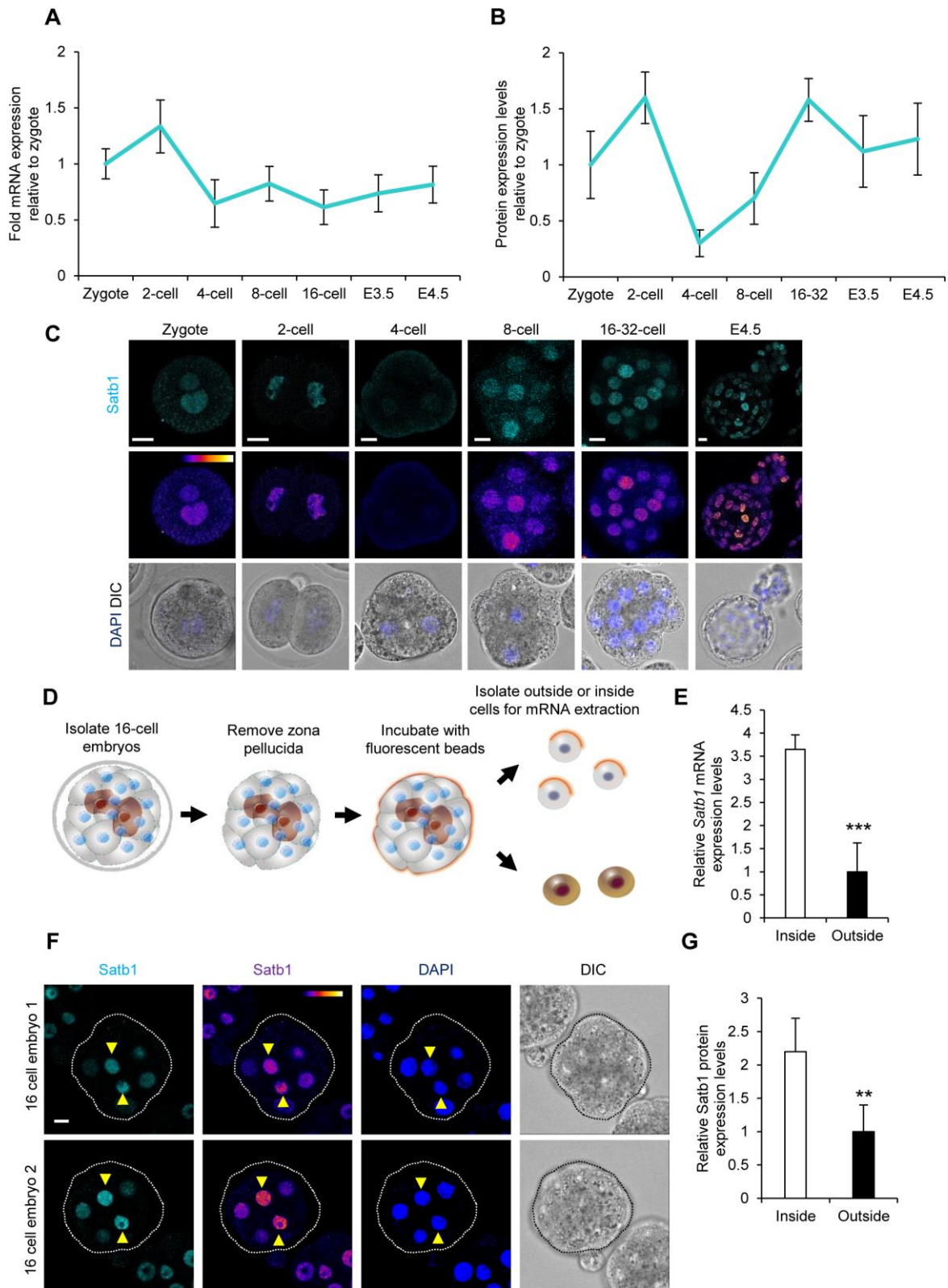


**Figure 1. Satb1 expression throughout preimplantation development.** A) qRT-PCR of embryos at zygote (n=42), two-cell (n=43), four-cell (n=39), 8-cell (n=41), 16-cell (n=41), E3.5 (n=54) and E4.5 (n=56) to investigate Satb1 mRNA levels. B) Quantification of relative fluorescent intensity of Satb1 staining throughout preimplantation development. Representative images presented in C. C) Immunofluorescence of Satb1 in zygote (n=14), two-cell (n=11), four-cell (n=12), 8-cell (n=15), 16-32 cell (n=13), E3.5 (n=15) and E4.5 (n=16) embryos. D) Scheme of isolation of inside and outside cells at the 16-cell stage for qRT-PCR shown in E. E) qRT-PCR of inside (n=35 cells,) and outside (n=41 cells,) cells from 16-cell stage embryos to investigate Satb1 mRNA levels. F) Immunofluorescence of Satb1 in 16-cell embryos (n=13). Embryo boundary is outlined in white or black. Inside cells indicated by yellow arrows. G) Quantification of relative fluorescent intensity of Satb1 staining. Representative images shown in F.

Scale bars, 10  $\mu$ m.



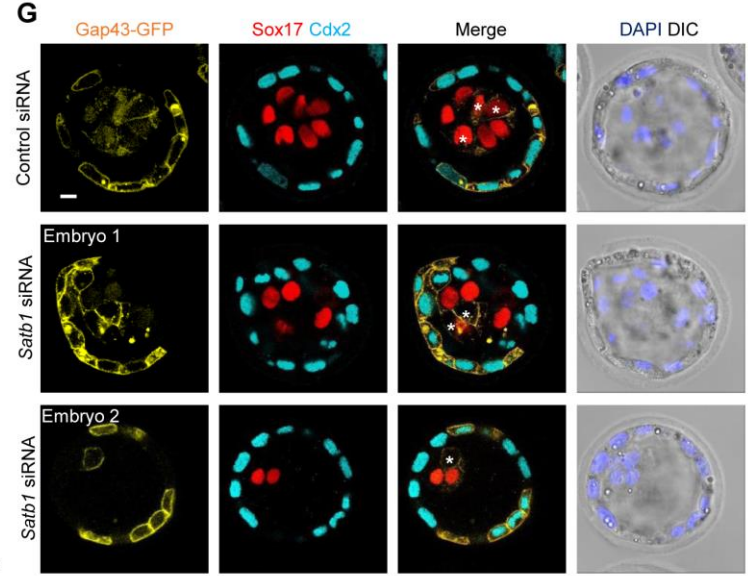
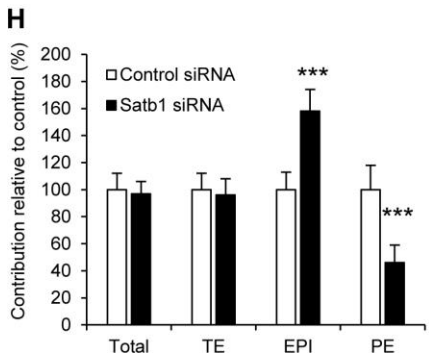
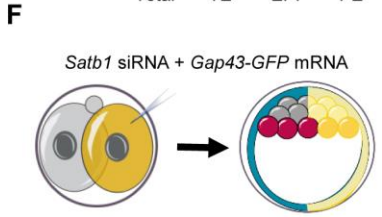
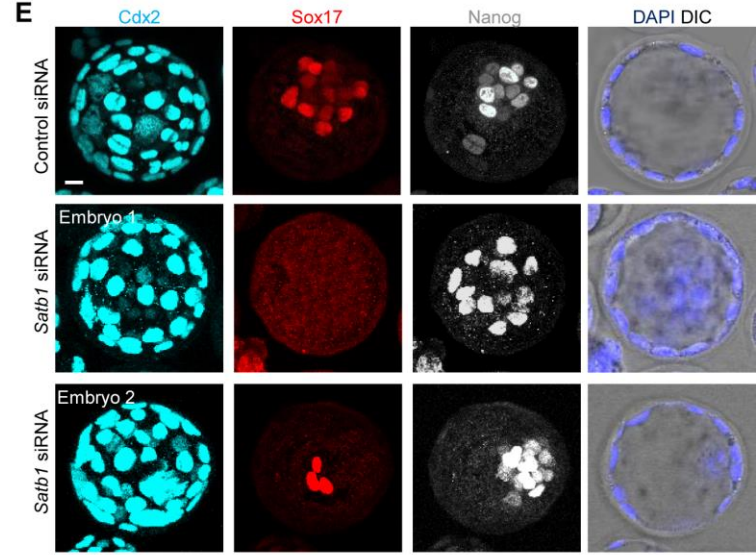
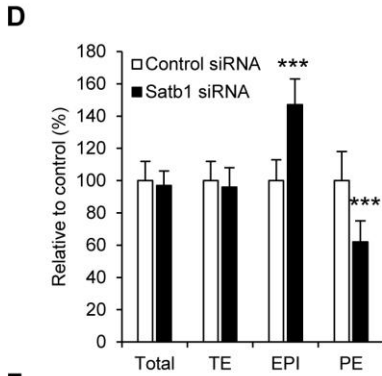
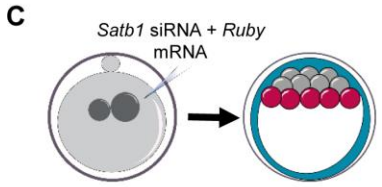
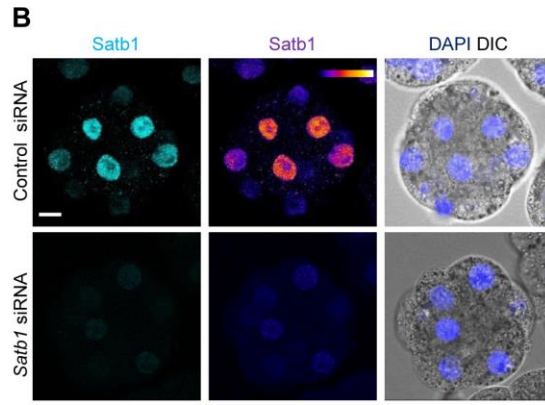
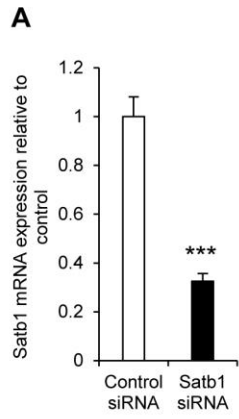


**Figure 2 Reducing *Satb1* biases ICM cell fate towards EPI over PE.** A) qRT–PCR of control siRNA (n=52 embryos, three biological repeats) and *Satb1* siRNA (n=61 embryos, three biological repeats) injected embryos to investigate *Satb1* mRNA levels. Embryos were injected at zygote and isolated at the 8-cell stage. Embryos injected with *Satb1* siRNA show a reduction in *Satb1* mRNA by the 8-cell stage. B) Immunofluorescence of *Satb1* in 8-cell embryos after being injected with control (n=11) or *Satb1* siRNA (n=15) C) Scheme of *Satb1* siRNA experiment shown in D and E. Zygotes were injected with *Satb1* siRNA, or control siRNA and cultured until E4.5. D) Contribution of control (n=29) and *Satb1* (n=36) siRNA injected embryos to EPI, PE, and TE. Representative images of the experiment are shown in E, E) Confocal images of control and *Satb1* siRNA injected embryos. *Nanog*, (EPI), *Sox17* (PE) and *Cdx2* (TE) were used as lineage markers. Related to Figure S2 F) Scheme of clonal *Satb1* siRNA experiment shown in G and H. One blastomere of two-cell stage embryos was injected with *Satb1* siRNA, or control siRNA, and *Gap43-GFP* mRNA. Embryos were cultured to the late blastocyst stage and the contribution of the injected cells' progeny to each lineage analysed. G) Confocal images of control (n=21, average of 5.2 *Sox17*+ve/*Gap43-GFP*-ve and an average of 4.96 *Sox17*+ve/*Gap43-GFP*+ve blastomeres per embryo) and *Satb1* (n=29, average of 7.84 *Sox17*+ve/*Gap43-GFP*-ve and an average of 2.28 *Sox17*+ve/*Gap43-GFP*+ve blastomeres per embryo) siRNA injected embryos. *Sox17* (PE) and *Cdx2* (TE) were used as lineage markers. Asterisks indicate ICM cells contributed from injected blastomeres. H) Contribution of *Satb1* siRNA injected cells from experiment shown in G to TE, PE and EPI, relative to control siRNA injected cells.

Scale bars, 10  $\mu$ m.



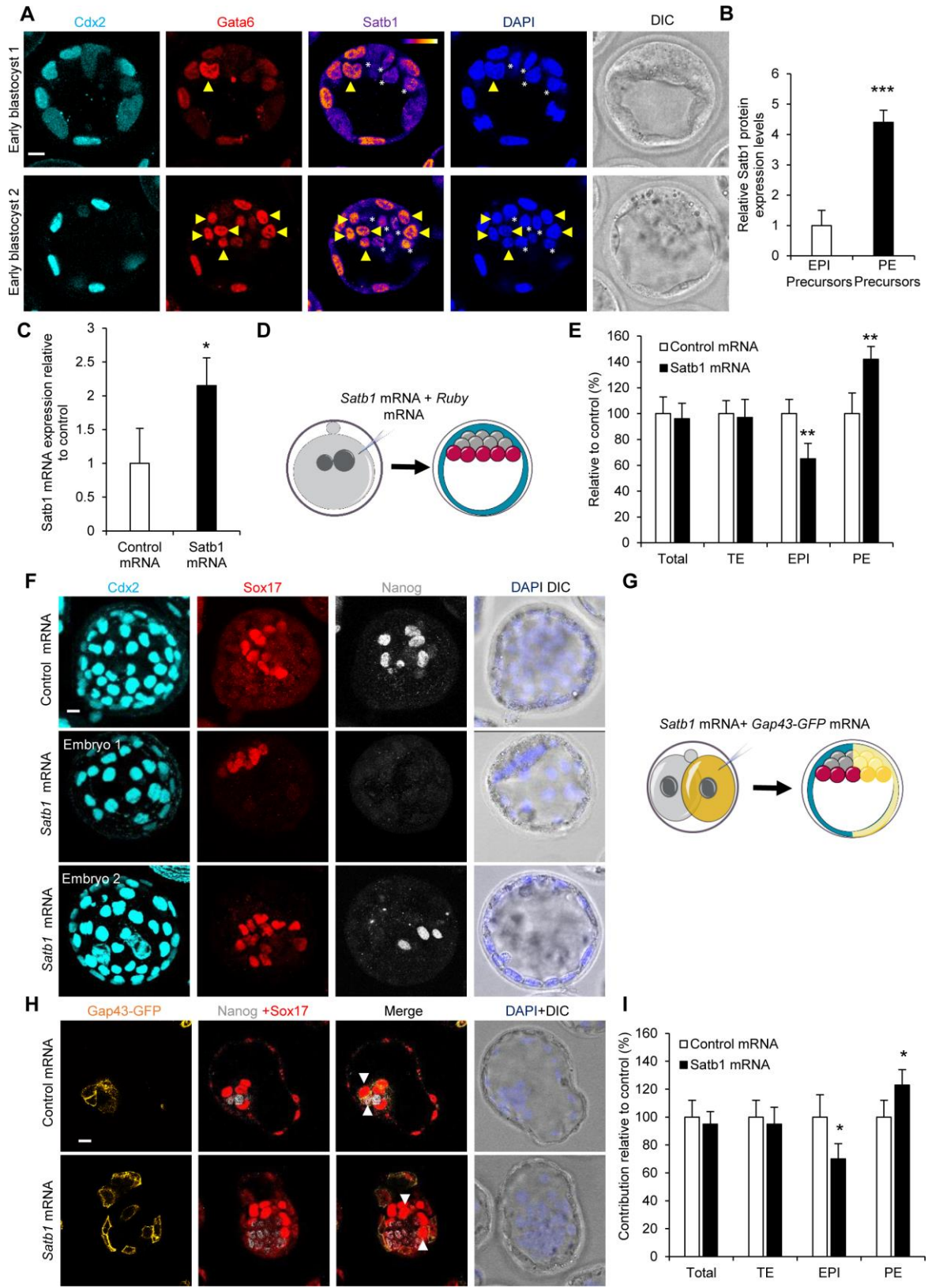


**Figure 3. Effect of Satb1 overexpression on preimplantation development.** A) Confocal images of Satb1 staining in early blastocysts (n=19). Gata6 (PE) Cdx2 (TE) used as lineage markers. Yellow arrows indicate PE precursors. White asterisks indicate EPI precursors. B) Quantification of relative fluorescent intensity of Satb1 staining from A. C) qRT-PCR of control mRNA (n=42 embryos) and Satb1 mRNA (n=54 embryos) injected embryos to investigate Satb1 mRNA levels. D) Scheme of Satb1 overexpression experiment shown in E and F. Zygotes were injected with Satb1 mRNA, or control mRNA and cultured until E4.5. E) Contribution of Satb1 mRNA (n=23) injected embryos to TE, PE and EPI, relative to control mRNA (n=25) injected cells. Representative images of the experiment are shown in F. F) Confocal images of control and Satb1 mRNA injected embryos. Nanog (EPI), Sox17 (PE) and Cdx2 (TE) were used as lineage markers. G) Scheme of clonal Satb1 mRNA experiment shown in H and I. One blastomere of two-cell stage embryos was injected with Satb1 mRNA and *Gap43-GFP* mRNA. Embryos were cultured to the late blastocyst stage and the contribution of the injected cells' progeny to each lineage analysed. H) Confocal images of control (n=19, average of 5.32 Nanog+ve/Gap43-GFP-ve and an average of 5.16 Nanog+ve/Gap43-GFP+ve blastomeres per embryo) and Satb1 (n=26, average of 7.27 Nanog+ve/Gap43-GFP-ve and an average of 3.61 Nanog+ve/Gap43-GFP+ve blastomeres per embryo) mRNA injected embryos. Sox17 (PE) and Nanog (EPI) were used as lineage markers. Arrows indicate ICM cells contributed from injected blastomeres. I) Contribution of Satb1 mRNA injected cells from experiment shown in H to TE, PE and EPI, relative to control mRNA injected cells.

Scale bars, 10  $\mu$ m.

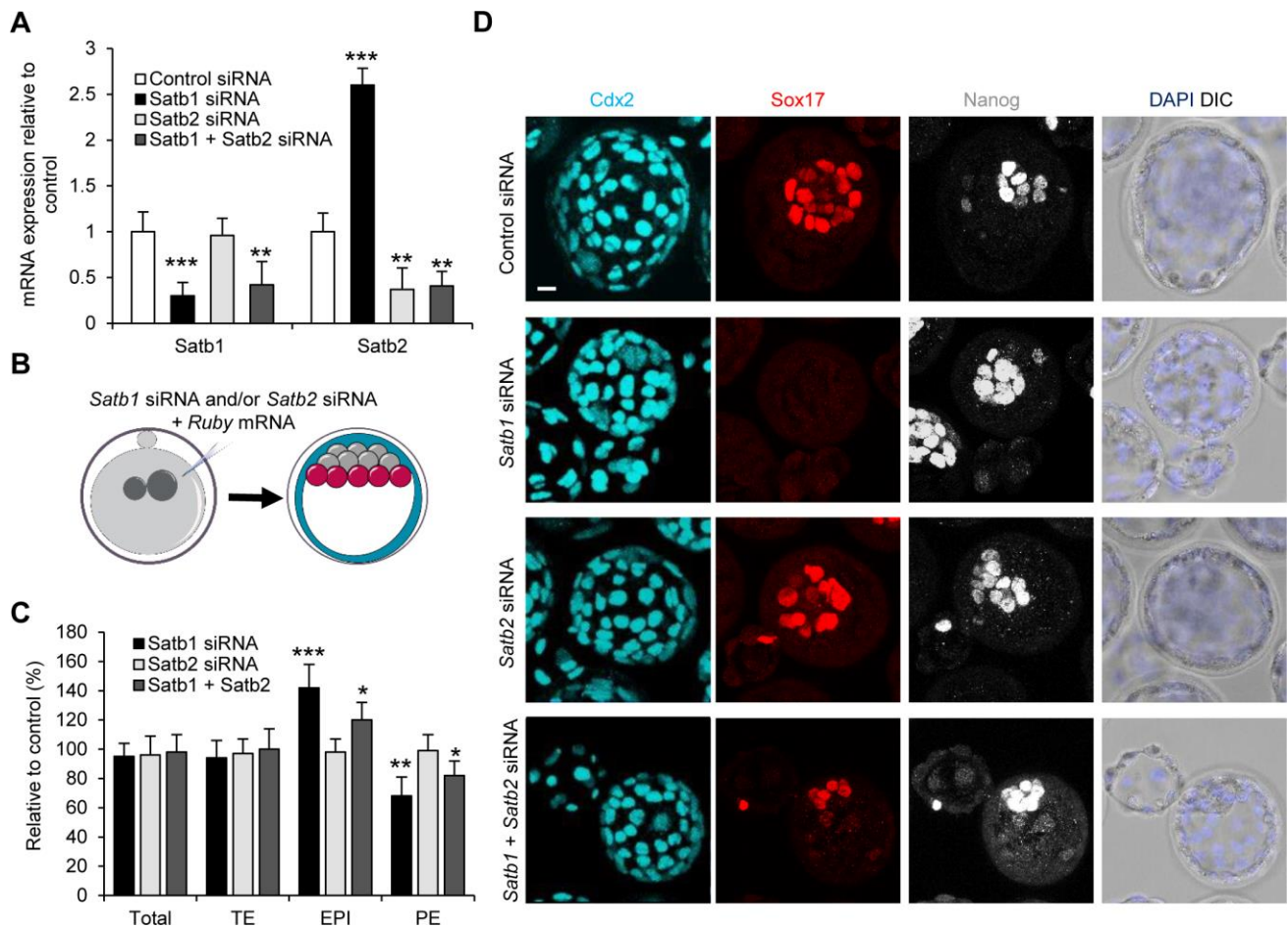


**Figure 4 Rescue of Satb1 siRNA phenotype by Satb2 siRNA.** A) qRT-PCR of control (n=39 embryos), Satb1 (n=52 embryos), Satb2 (n=64 embryos), Satb1 + Satb2 (n=52 embryos) siRNA injected embryos to investigate Satb1 mRNA levels. B) Scheme of Satb1 and Satb1 siRNA experiment shown in C and D. Zygotes were injected with Satb1 siRNA and/or Satb2 siRNA and cultured until E4.5. C) Contribution of Satb1 (n=16), Satb2 (n=29) and Satb1 + Satb2 (n=32) siRNA injected embryos to TE, PE and EPI, relative to control (control numbers were normalised to 100, to allow comparison with siRNA injected embryos) (n=13) siRNA injected cells (not shown). Representative images of the experiment are shown in D. D) Confocal images of control, Satb1, Satb2, and Satb1+Satb2 siRNA injected embryos. Nanog (EPI), Sox17 (PE) and Cdx2 (TE) were used as lineage markers. Scale bar, 10  $\mu$ m.

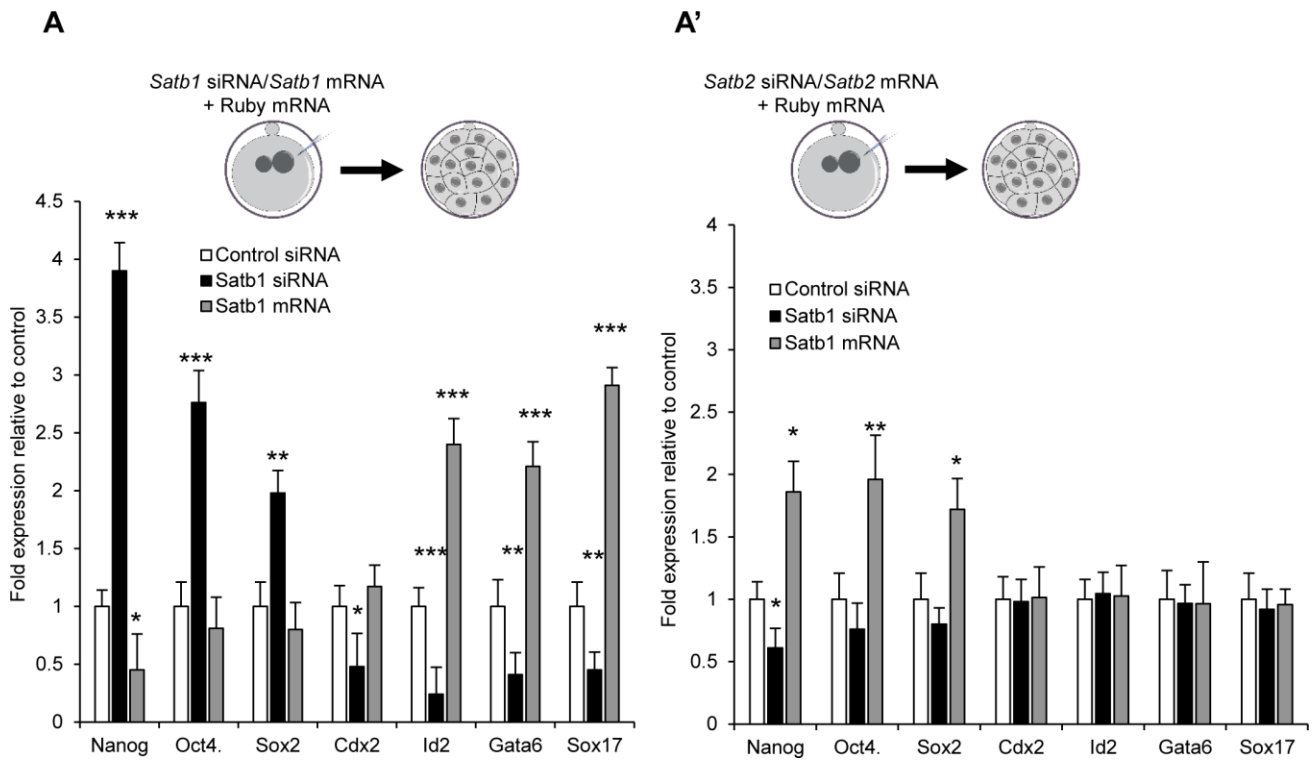


**Figure 5. Gene expression changes after modulating *Satb1* and *Satb2*.** A) qRT-PCR of control siRNA (n=59 embryos), *Satb1* siRNA (n=62 embryos), *Satb1* mRNA (n=71 embryos) for various genes. A') qRT-PCR of control siRNA (n=59 embryos), *Satb2* siRNA (n=73 embryos), and *Satb2* mRNA (n=58 embryos) for various genes. In both cases zygotes were injected and cultured until morula.



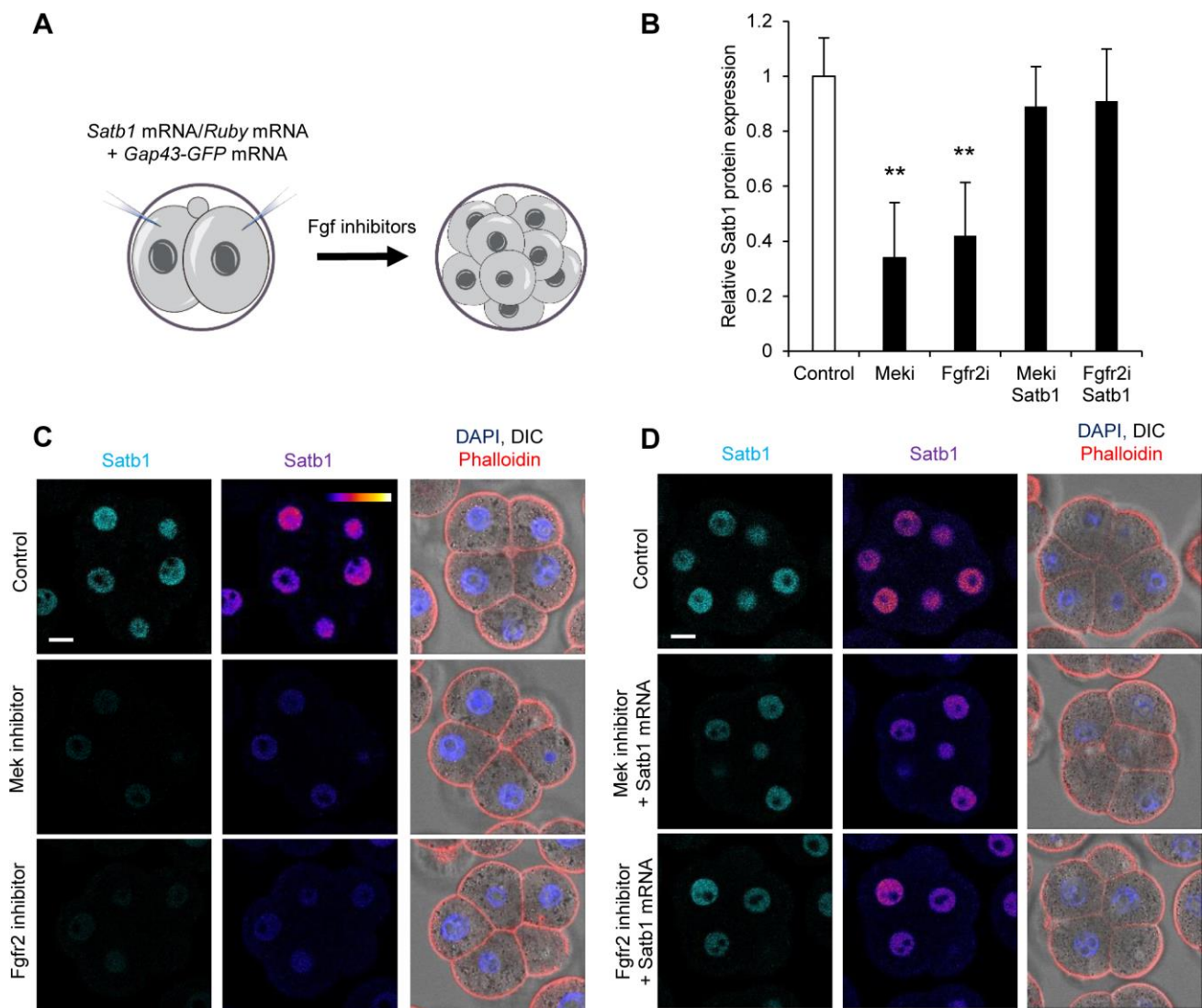


**Figure 6. The effect of Fgf signalling on Satb1 expression.** A) Scheme of Fgf inhibition experiments in B, C and D. Two-cell stage embryos were either injected with *Satb1* mRNA or Ruby mRNA and treated with a Fgf signalling inhibitor or left untreated before isolation at the 8-cell stage for analysis. B) Quantification of relative fluorescent intensity of Satb1 staining from C and D. C) Confocal images of control (n=18), Mek inhibitor (n=20), and Fgfr2 inhibitor (n=22) treated embryos. D) Confocal images of control (n=18), Mek inhibitor treated + injected with *Satb1* mRNA (n=17), and Fgfr2 inhibitor treated + injected with *Satb1* mRNA (n=15) embryos.

Scale bars, 10  $\mu$ m.

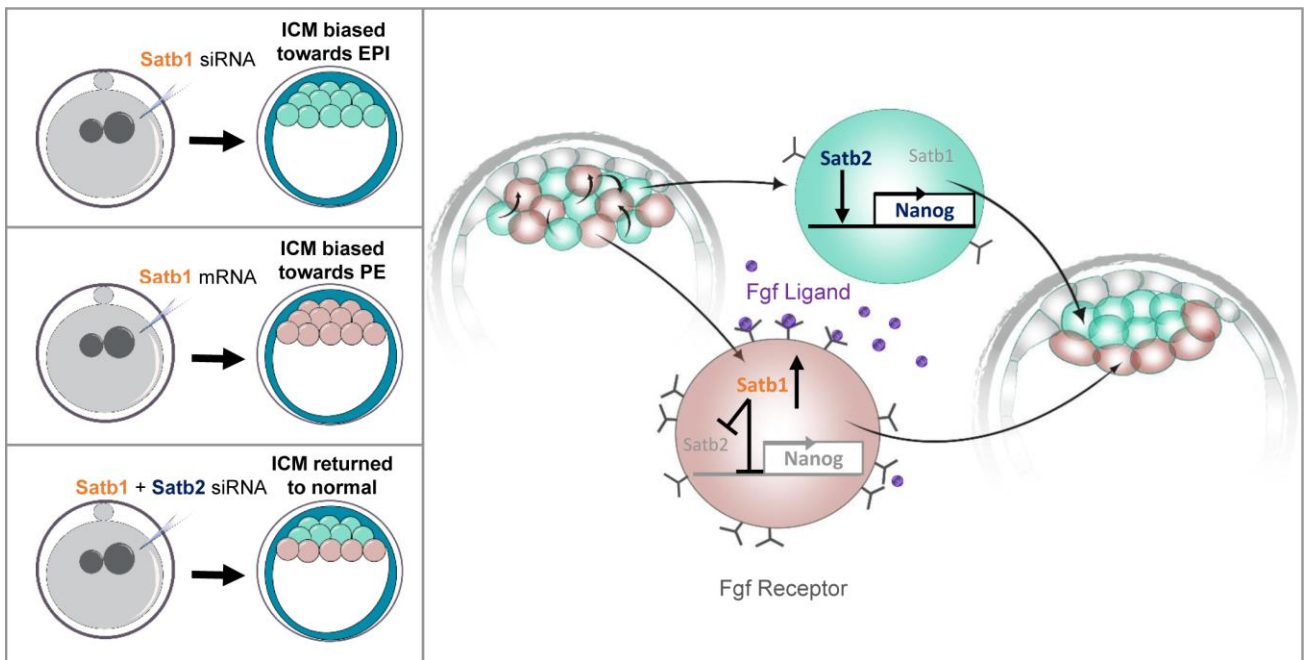


**Figure 7. Model for the role of Satb1 in ICM lineage segregation.** A ‘salt and pepper’ distribution of Fgfr2 by the 64-cell stage means different cells have different responses to Fgf4 signalling. Cells with lower levels of Fgfr2 are less susceptible to Fgf4 signalling and do not upregulate Satb1. Nanog is therefore more highly expressed promoting the formation of EPI. When Satb1 is knocked down using a specific siRNA there is an increase in Nanog and therefore an increase in the number of EPI cells present in the embryo. Conversely, cells that are more susceptible to Fgf4 signalling have higher levels of Satb1. Higher expression of Satb1 leads to the inhibition of *Nanog* and *Satb2*. This in turn leads these cells to differentiate into PE. Overexpression of Satb1 with an mRNA is similarly able to bias cell fate towards the PE lineage. Reducing both Satb1 and Satb1 simultaneously is able to restore the balance in PE and EPI by removing both an activator and repressor of Nanog.

## Supplementary Materials and Methods

### siRNA sequences

The sequences of the siRNAs used are as follows: Satb1 siRNA 1– AAGGTGGTACAAACATTTCAA, Satb1 siRNA 2– CAGGAAATGAAGCGTGCTAAA, Satb1 siRNA 3 – CCCGAAGTACACCATCATCAA, Satb2 siRNA 1 – CCGAAGGACTAGACTGTGAA, Satb2 siRNA 2–ATGGCCCATCTGATAAACCAA, Satb2 siRNA 3–CAGGGATTATTGTCAGAGATA.

### Immunofluorescence protocol and intensity measurements and antibody details

ICM cells were identified through sequential scanning through embryo z-stacks by their position as well as through the use of lineage markers. Nanog expressing cells in the ICM that did not express PE markers were identified as EPI. Inside and outside cells were identified by careful scanning through the z-stack. Only in cases when outer (with nuclei that were not surrounded by other cells and adjacent to the outside of the embryo) and inner (with nuclei that were entirely surrounded by other cells) cells could be unambiguously identified where they used for analyses. Fluorescence intensity was quantified by normalising to DAPI and layer-normalising using the built-in IMAGEJ function. Intensity measurements were done on the normalised sections using the IMAGEJ measure function. For antibody details see Supplementary Materials and Methods. Primary antibodies used: goat anti-Sox17 (1:200; R&D Systems, AF1924), goat anti-Pdgfra (1:200; Santa Cruz, sc-31178), goat anti-Gata6 (1:200; R&D Systems, AF1700), rabbit anti-Nanog (1:200; Abcam, AB80892), rabbit anti-Sox2 (1:200; Abcam, ab59776), rabbit anti-Sox2 (1:200; Millipore, AB5603) mouse anti-Cdx2 (1:200; Biogenex, AM392), rabbit anti-Satb1 (1:50; Abcam, AB49061), rabbit anti-Satb2 (1:200; Abcam, AB34735), rat anti-Nanog (1:200; Ebiosciences, 14-5761-80). Secondary antibodies used: Alexa Fluor 647 donkey anti-mouse IgG, Alexa Fluor 568 donkey anti-goat IgG, Alexa Fluor 568 donkey anti-rabbit IgG, Alexa Fluor 647 donkey anti-rabbit IgG, Alexa Fluor 647 donkey anti-goat IgG, Alexa Fluor 647 phalloidin.

### Primer details

The following primers were used all written 5'-3': Gapdh Forward, AGAGACGGCCGCATCTTC, Reverse, CCCAATACGGCCAAATCCGT'; Histone H2A.Z Forward, CGTCAGAGAGACGCTTACCG, Reverse, AAGCCTCCAACTTGCTCAAA; Satb1 Forward, AGTGCCCCCTTTCACAGAG, Reverse, TGCTGCTGAGACATTTGCAT; Satb2



Forward, ATGAACCCCAATGTGAGCAT, Reverse, GTTGTCGGTGTGCGAGGTTTT; Cdx2  
Forward, AACCTGTGCGAGTGGATG, Reverse, TCTGTGTACACCACCCGGTA; Nanog  
Forward, GGTTGAAGACTAGCAATGGTCTGA, Reverse, TGCAATGGATGCTGGGATACT;  
Oct3 Forward, TTGGGCTAGAGAAGGATGTGGTT, Reverse,  
GGAAAAGGGACTGAGTAGAG TGTGG; Sox2 primer set 1 Forward,  
GCGGAGTGGAACTTTTGTCC, Reverse, CGGGAAGCGTGTACTTATCCTT; Sox2 primer  
set 2 Forward, GCGGAGTGGAACTTTTGTCC Reverse,  
GGGAAGCGTGTACTTATCCTTCT; Sox17 Forward, GATGCGGGATACGCCAGTG,  
Reverse, CCACCACCTCGCCTTTCAC; Id2 Forward, ATGAAAGCCTTCAGTCCGGTG,  
Reverse, AGCAGACTCATCGGGTCGT; Gata6 Forward, TTGCTCCGGTAACAGCAGTG,  
Reverse, GTGGTCGCTTGTGTAGAAGGA

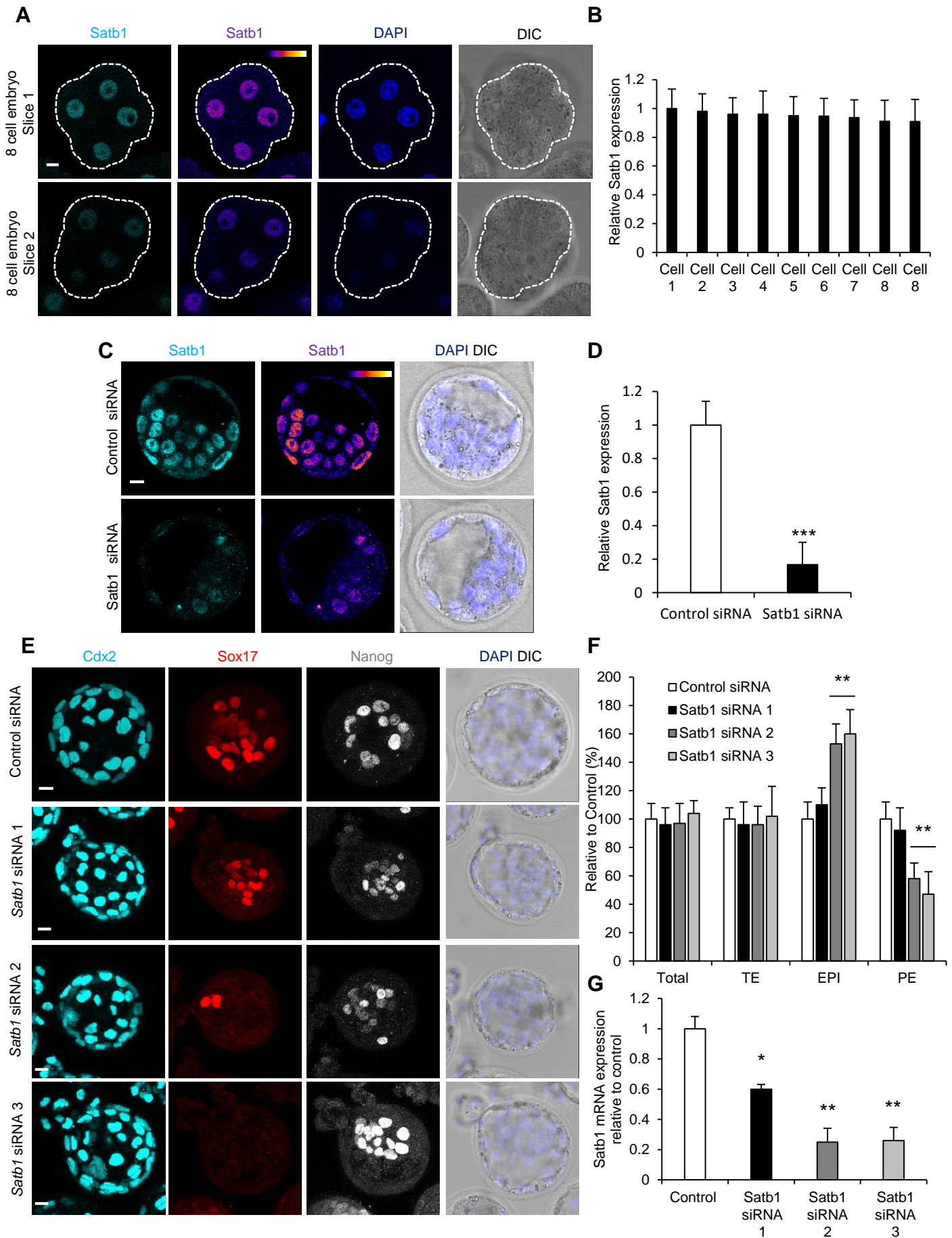


**Figure S1. Confirmation of *Satb1* siRNA persistence and specificity and *Satb1* embryo staining.** A) Immunofluorescence of *Satb1* in 8-cell embryos (n=25). Embryo boundary is outlined in white. B) Quantification of immunofluorescence represented in A. Fluorescence quantified and normalized to the nucleus with the strongest staining per individual embryo. C) Immunofluorescence of *Satb1* in early blastocysts after being injected with control (n=14) or *Satb1* siRNA (n=18). D) Quantification of relative fluorescent intensity of *Satb1* staining from C. E) Confocal images of control and *Satb1* siRNA 1, *Satb1* siRNA 2 and *Satb1* siRNA 3 injected embryos. *Nanog*, (EPI), *Sox17* (PE) and *Cdx2* (TE) were used as lineage markers. Quantification of this experiment shown in F. F) Contribution of control (n=17) and *Satb1* siRNA 1 (n=19), 2 (n=21), and 3 (n=23) injected embryos to EPI, PE, and TE. G) qRT-PCR of control (n=47 embryos, three biological repeats), *Satb1* siRNA 1 (n=58 embryos, three biological repeats), *Satb1* siRNA 2 (n=53 embryos, three biological repeats), *Satb1* siRNA 3 (n=49 embryos, three biological repeats) injected embryos to investigate *Satb1* mRNA levels. Student's t-test was used to test significance \*= p<0.05, \*\*= p<0.01, \*\*\*= p<0.001. Error bars represent s.e.m. Scale bars, 10  $\mu$ m.

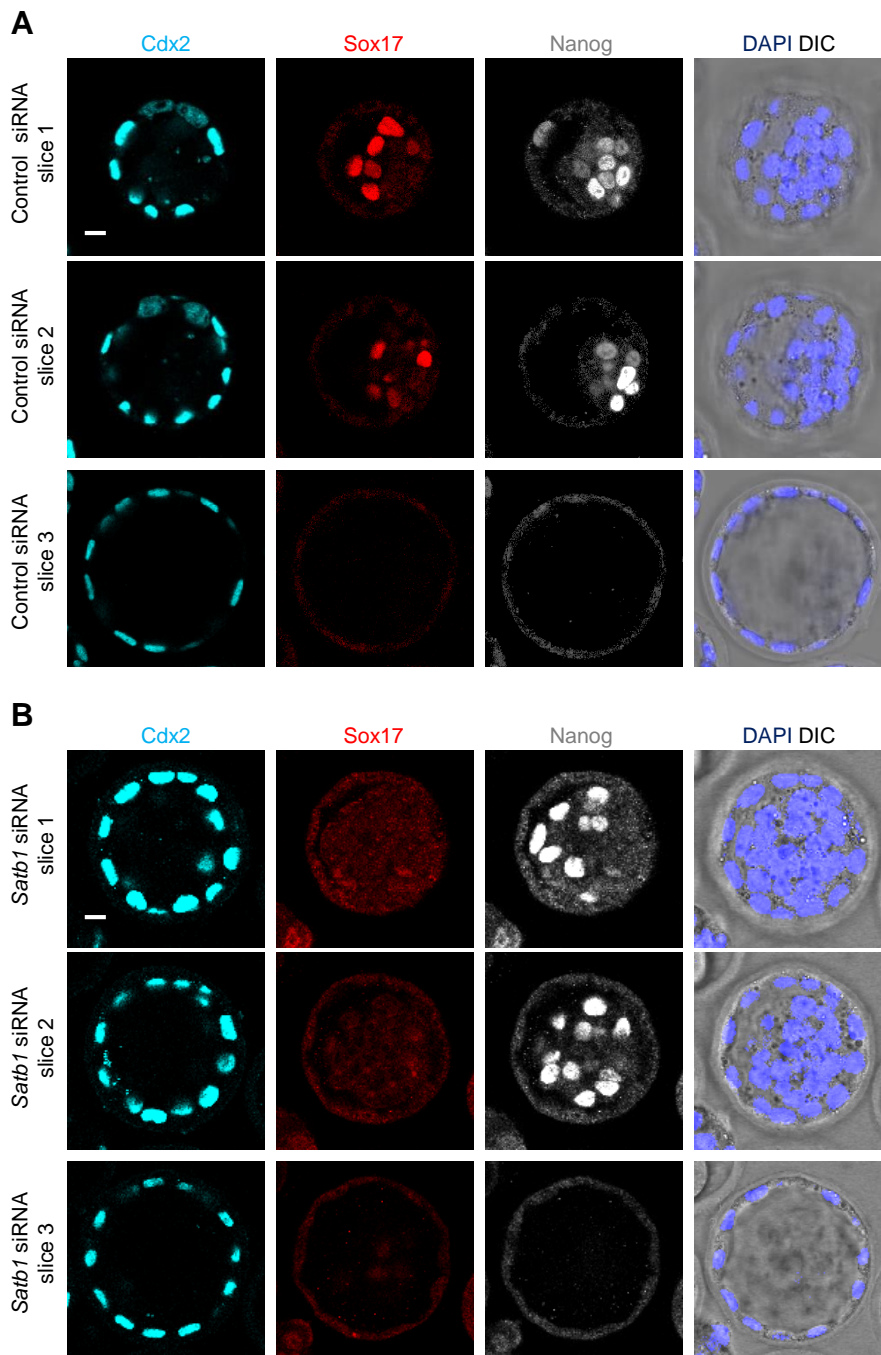


**Figure S2. Z-stack slices of confocal images from Figure 2E.** A) Slices of the confocal z-stack of the control siRNA injected embryo presented in Fig 2 E. Nanog, (EPI), Sox17 (PE) and Cdx2 (TE) were used as lineage markers B) Slices of the confocal Z-stack of the Satb1 siRNA injected embryo presented in Fig 2 E (Embryo 1). Nanog, (EPI), Sox17 (PE) and Cdx2 (TE) were used as lineage markers. Scale bars, 10  $\mu$ m.



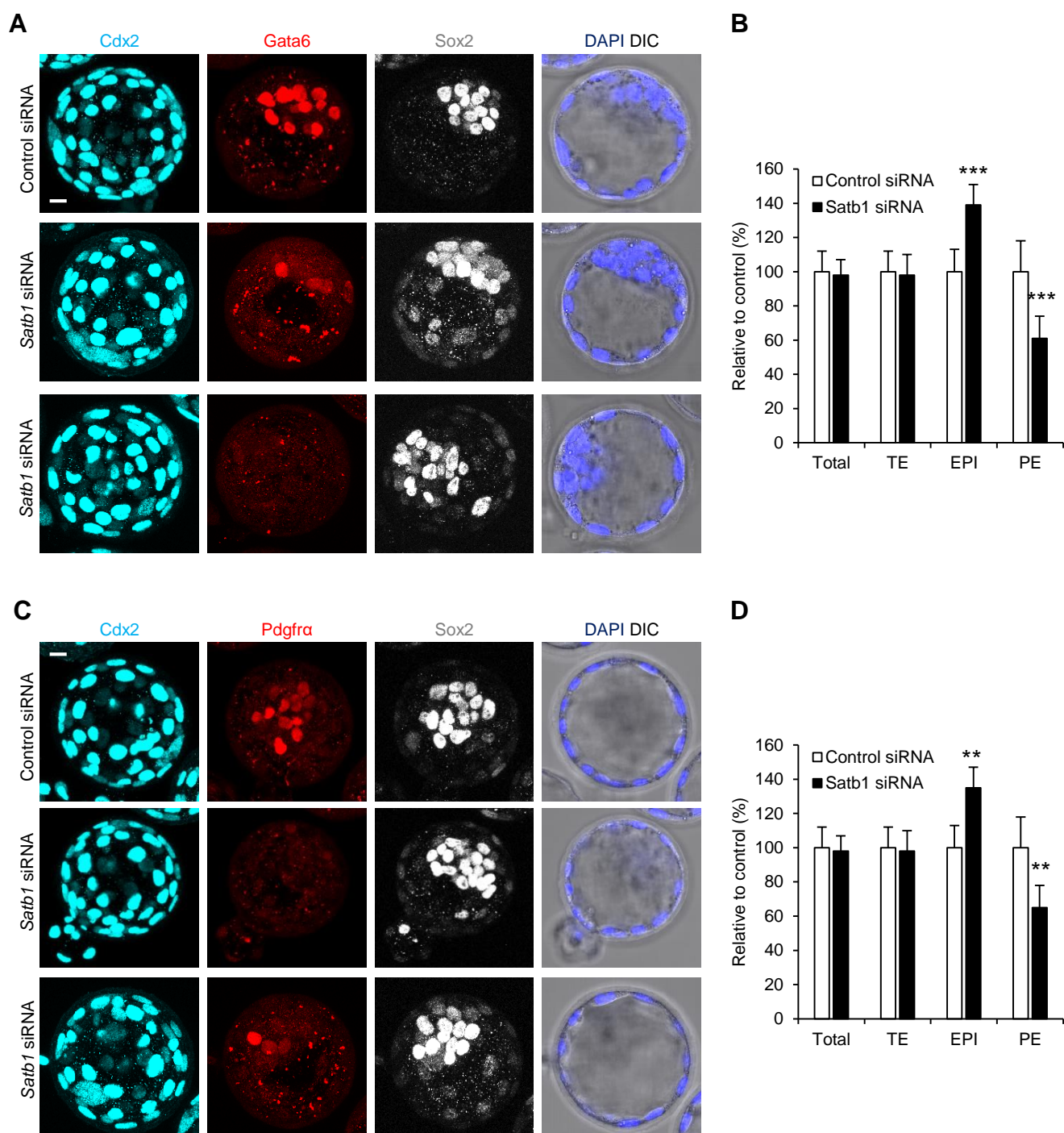


**Figure S3. *Satb1* siRNA phenotype assessed by Sox2, Gata6 and Pdgfra.** A) Confocal images of control (n=31) and *Satb1* siRNA (n=30) injected embryos. Sox2, (EPI), Gata6 (PE) and Cdx2 (TE) were used as lineage markers. B) Contribution of control and *Satb1* siRNA injected embryos represented in A to EPI, PE, and TE. C) Confocal images of control (n=27) and *Satb1* siRNA (n=29) injected embryos. Sox2, (EPI), Pdgfra (PE) and Cdx2 (TE) were used as lineage markers. D) Contribution of control and *Satb1* siRNA injected embryos represented in C to EPI, PE, and TE.

Student's t-test was used to test significance \*= p<0.05, \*\*= p<0.01. Error bars represent s.e.m. Scale bars, 10  $\mu$ m.

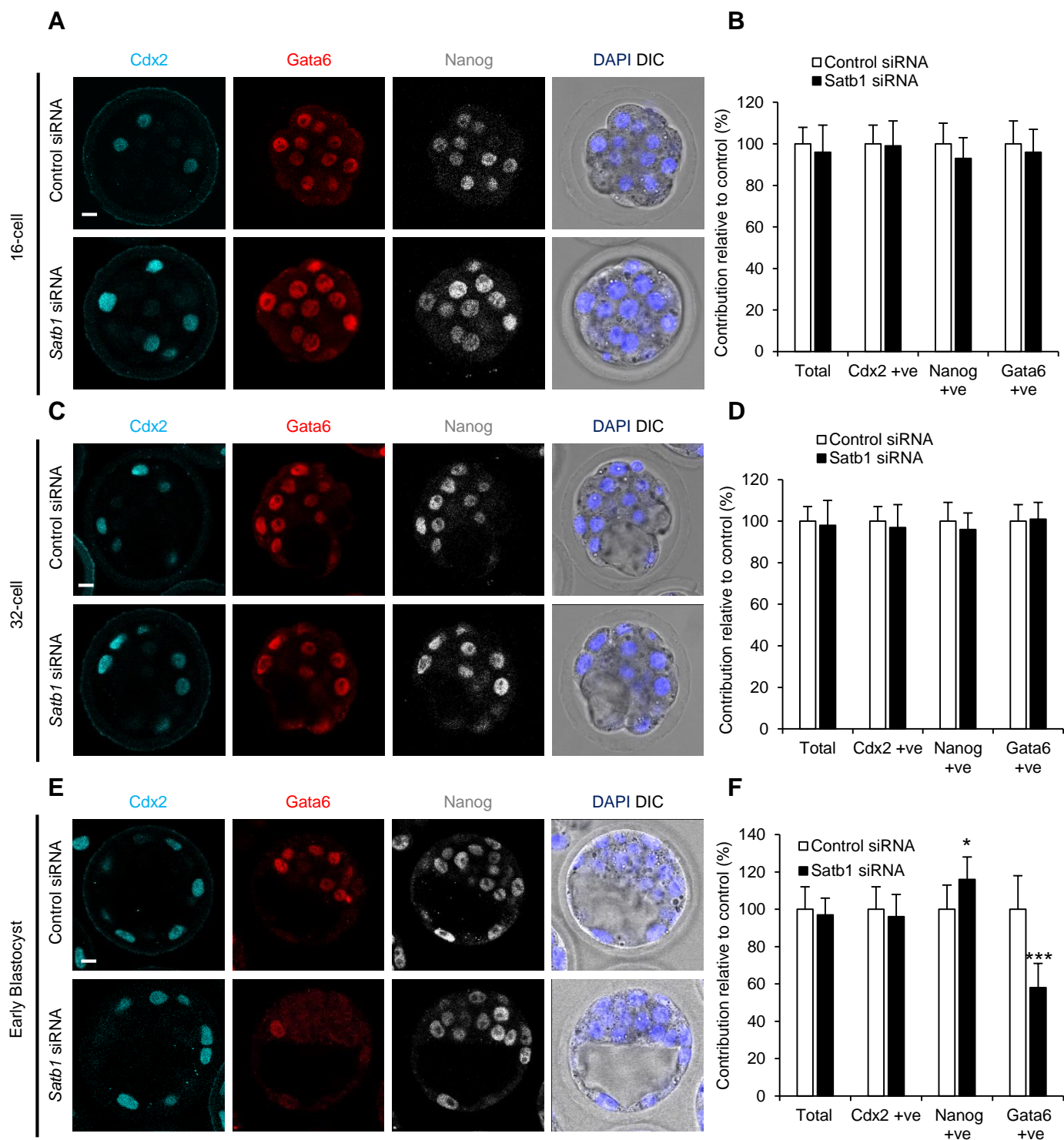


**Figure S4. Timing of effect of *Satb1* RNAi.** A) Confocal images of control (n=15) and *Satb1* siRNA (n=21) injected embryos at the 16-cell stage showing the localisation and distribution of Cdx2, Gata6 and Nanog. B) Relative number of blastomeres that are positive for Cdx2, Nanog and Gata6 from control and *Satb1* siRNA injected embryos represented in A. C) Confocal images of control (n=17) and *Satb1* siRNA (n=19) injected embryos at the 32-cell stage showing the localisation and distribution of Cdx2, Gata6 and Nanog. D) Relative number of blastomeres that are positive for Cdx2, Nanog and Gata6 from control and *Satb1* siRNA injected embryos represented in C. E) Confocal images of control (n=19) and *Satb1* siRNA (n=28) injected embryos at the early blastocyst stage showing the localisation and distribution of Cdx2, Gata6 and Nanog. F) Relative number of blastomeres that are positive for Cdx2, Nanog and Gata6 from control and *Satb1* siRNA injected embryos represented in E. Student's t-test was used to test significance \*= p<0.005, \*\*\*= p<0.001. Error bars represent s.e.m. Scale bars, 10  $\mu$ m.

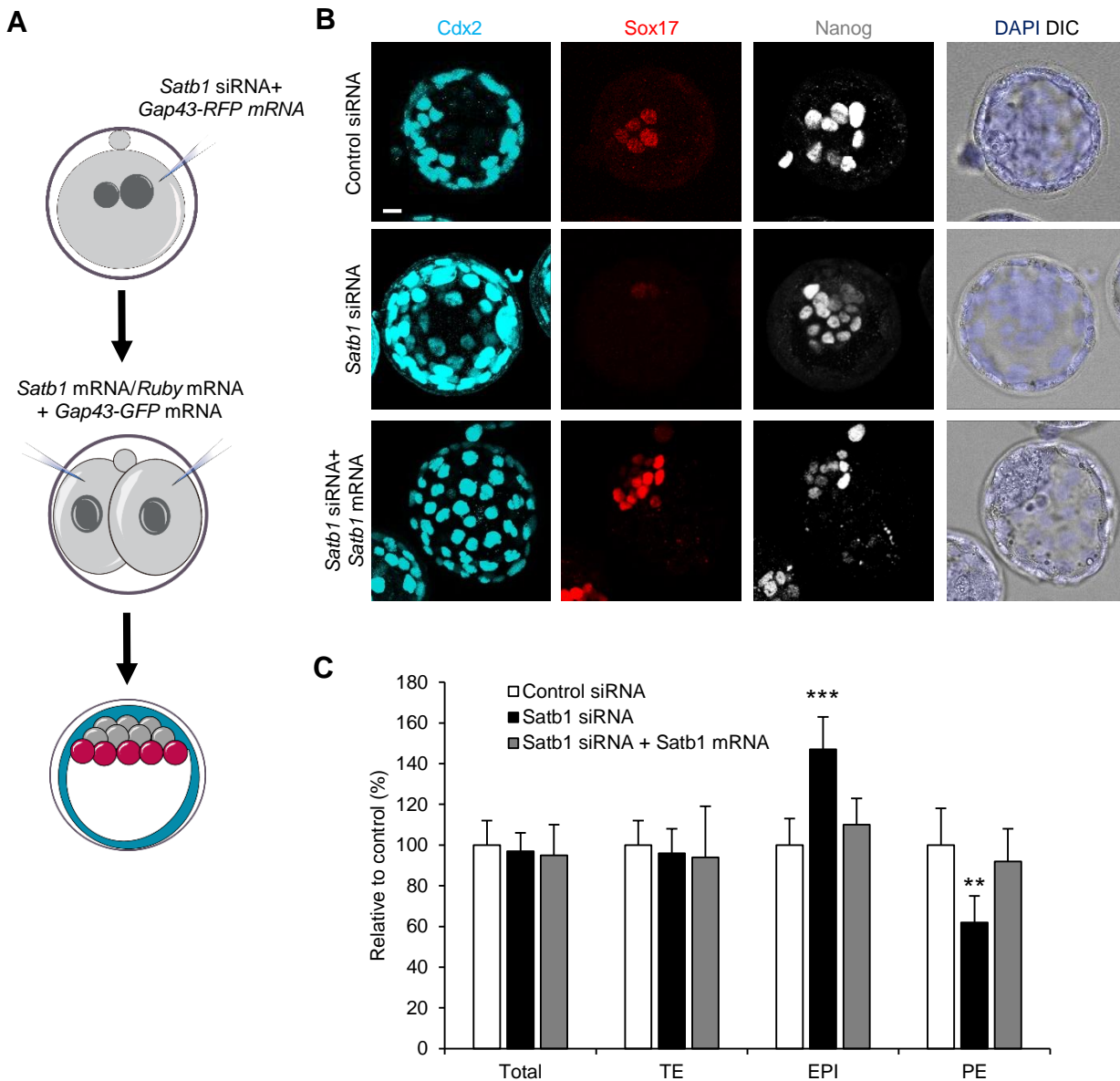


**Figure S5. Rescue of *Satb1* siRNA phenotype by *Satb1* mRNA.** A) Scheme of *Satb1* rescue experiment shown in B and C. Zygotes were injected with *Satb1* siRNA or control siRNA. At the 2-cell stage both blastomeres were then injected with either *Satb1* mRNA or *Ruby* mRNA as a control and then cultured until E4.5. B) Confocal images of control siRNA (n=12), *Satb1* siRNA (n=21) and *Satb1* siRNA + *Satb1* mRNA (n=26) injected embryos. Nanog (EPI), Sox17 (PE) and Cdx2 (TE) were used as lineage markers. C) Contribution of *Satb1* siRNA and *Satb1* siRNA + *Satb1* mRNA injected embryos to TE, PE and EPI, relative to control siRNA injected cells from experiment shown in B.

Student's t-test was used to test significance \*\*= p<0.01, \*\*\*= p<0.001. Error bars represent s.e.m. Scale bar, 10  $\mu$ m.



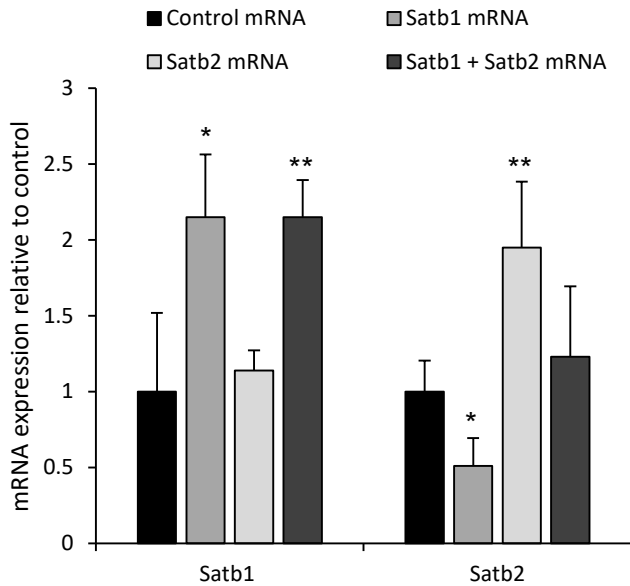


**Figure S6. Effect of Satb1 and Satb2 overexpression on Satb1 and Satb2 mRNA levels.** qRT-PCR of control (n=63 embryos, three biological repeats), Satb1 (n=71 embryos, three biological repeats), Satb2 (n=58 embryos, three biological repeats), Satb1 + Satb2 (n=47 embryos, three biological repeats) mRNA injected embryos to investigate Satb1 and Satb2 mRNA levels. Student's t-test was used to test significance \*\*=  $p < 0.01$ , \*\*\*=  $p < 0.001$ . Error bars represent s.e.m. Scale bar, 10  $\mu$ m.

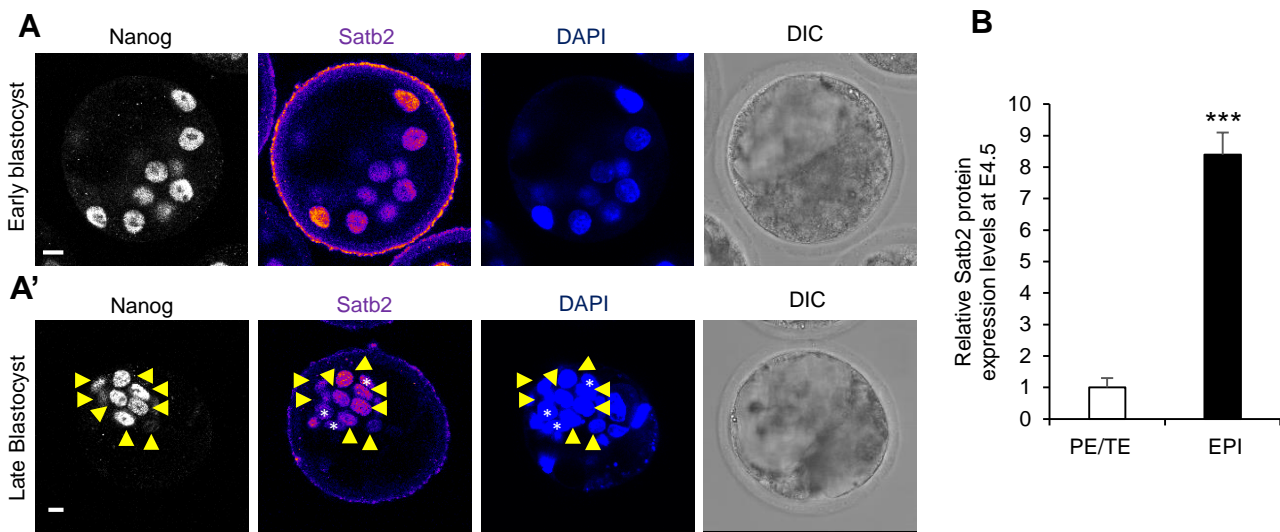


**Figure S7. Satb1 expression pattern in blastocysts.** A) Confocal images of Satb2 and Nanog staining in early blastocysts (n=12). A') Confocal images of Satb2 and Nanog staining in late blastocysts (n=16). Yellow arrows indicate EPI cells positive for Satb2. White asterisks indicate PE cells positive for Satb2. B) Quantification of relative fluorescent intensity of Satb2 staining in EPI cells compared to PE/TE cells in late blastocysts as shown in A'. EPI cells were identified by the expression of Nanog. Scale bars, 10  $\mu$ m.

## Supplementary Materials and Methods

### siRNA sequences

The sequences of the siRNAs used are as follows: Satb1 siRNA 1– AAGGTGGTACAAACATTTCAA, Satb1 siRNA 2– CAGGAAATGAAGCGTGCTAAA, Satb1 siRNA 3 – CCCGAAGTACACCATCATCAA, Satb2 siRNA 1 – CCGAAGGACTAGACTGTGAA, Satb2 siRNA 2–ATGGCCCATCTGATAAACCAA, Satb2 siRNA 3–CAGGGATTATTGTCAGAGATA.

### Immunofluorescence protocol and intensity measurements and antibody details

ICM cells were identified through sequential scanning through embryo z-stacks by their position as well as through the use of lineage markers. Nanog expressing cells in the ICM that did not express PE markers were identified as EPI. Inside and outside cells were identified by careful scanning through the z-stack. Only in cases when outer (with nuclei that were not surrounded by other cells and adjacent to the outside of the embryo) and inner (with nuclei that were entirely surrounded by other cells) cells could be unambiguously identified where they used for analyses. Fluorescence intensity was quantified by normalising to DAPI and layer-normalising using the built-in IMAGEJ function. Intensity measurements were done on the normalised sections using the IMAGEJ measure function. For antibody details see Supplementary Materials and Methods. Primary antibodies used: goat anti-Sox17 (1:200; R&D Systems, AF1924), goat anti-Pdgfra (1:200; Santa Cruz, sc-31178), goat anti-Gata6 (1:200; R&D Systems, AF1700), rabbit anti-Nanog (1:200; Abcam, AB80892), rabbit anti-Sox2 (1:200; Abcam, ab59776), rabbit anti-Sox2 (1:200; Millipore, AB5603) mouse anti-Cdx2 (1:200; Biogenex, AM392), rabbit anti-Satb1 (1:50; Abcam, AB49061), rabbit anti-Satb2 (1:200; Abcam, AB34735), rat anti-Nanog (1:200; Ebiosciences, 14-5761-80). Secondary antibodies used: Alexa Fluor 647 donkey anti-mouse IgG, Alexa Fluor 568 donkey anti-goat IgG, Alexa Fluor 568 donkey anti-rabbit IgG, Alexa Fluor 647 donkey anti-rabbit IgG, Alexa Fluor 647 donkey anti-goat IgG, Alexa Fluor 647 phalloidin.

### Primer details

The following primers were used all written 5'-3': Gapdh Forward, AGAGACGGCCGCATCTTC, Reverse, CCCAATACGGCCAAATCCGT'; Histone H2A.Z Forward, CGTCAGAGAGACGCTTACCG, Reverse, AAGCCTCCAACTTGCTCAAA; Satb1 Forward, AGTGCCCCCTTTCACAGAG, Reverse, TGCTGCTGAGACATTTGCAT; Satb2

Forward, ATGAACCCCAATGTGAGCAT, Reverse, GTTGTCGGTGTGCGAGGTTTT; Cdx2  
Forward, AACCTGTGCGAGTGGATG, Reverse, TCTGTGTACACCACCCGGTA; Nanog  
Forward, GGTTGAAGACTAGCAATGGTCTGA, Reverse, TGCAATGGATGCTGGGATACT;  
Oct3 Forward, TTGGGCTAGAGAAGGATGTGGTT, Reverse,  
GGAAAAGGGACTGAGTAGAG TGTGG; Sox2 primer set 1 Forward,  
GCGGAGTGGAACTTTTGTCC, Reverse, CGGGAAGCGTGTACTTATCCTT; Sox2 primer  
set 2 Forward, GCGGAGTGGAACTTTTGTCC Reverse,  
GGGAAGCGTGTACTTATCCTTCT; Sox17 Forward, GATGCGGGATACGCCAGTG,  
Reverse, CCACCACCTCGCCTTTCAC; Id2 Forward, ATGAAAGCCTTCAGTCCGGTG,  
Reverse, AGCAGACTCATCGGGTCGT; Gata6 Forward, TTGCTCCGGTAACAGCAGTG,  
Reverse, GTGGTCGCTTGTGTAGAAGGA

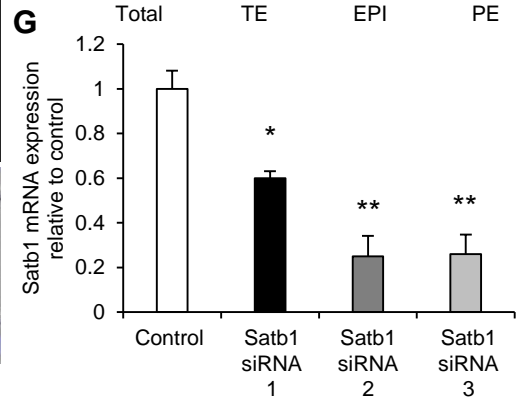
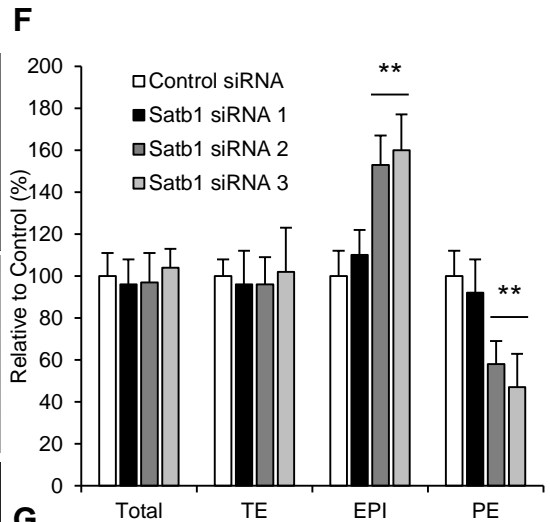
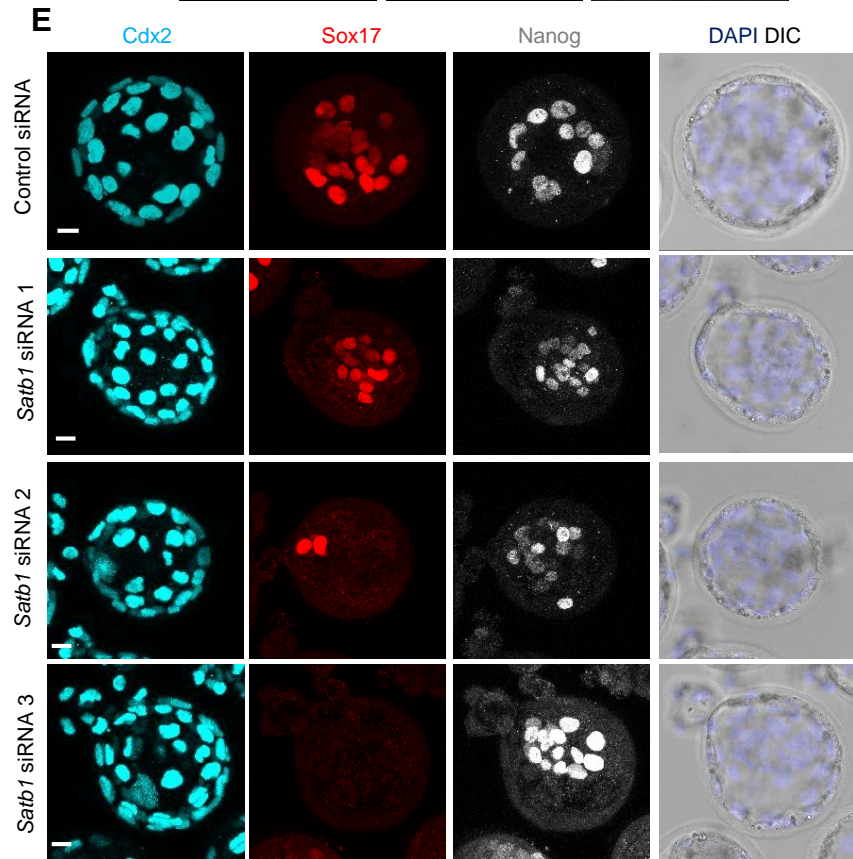
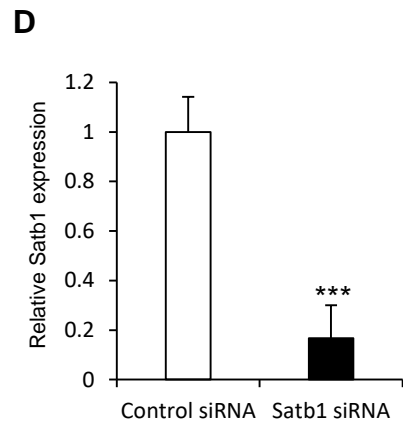
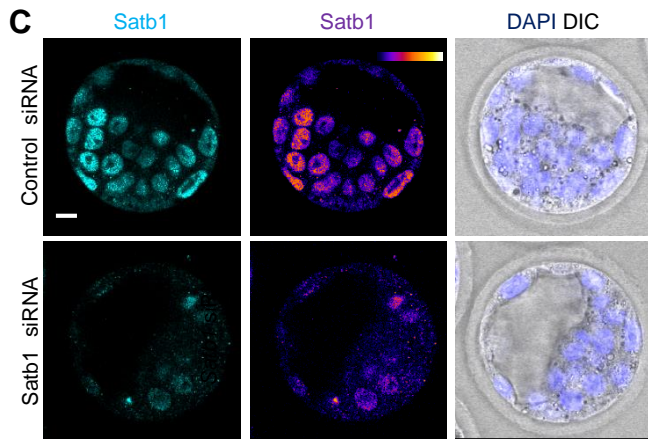
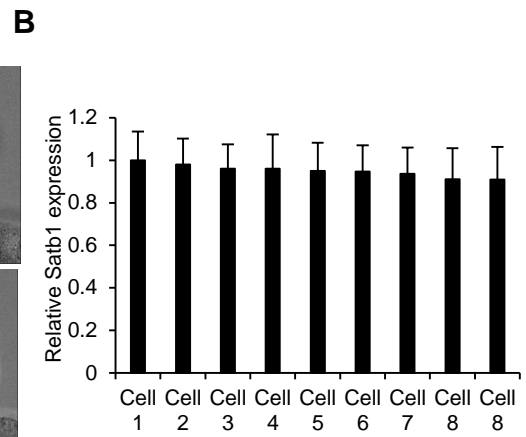
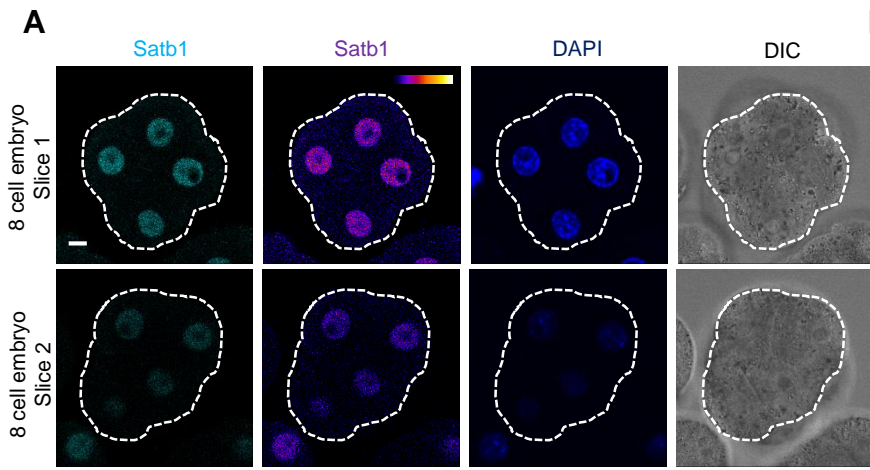


**Figure S1. Confirmation of *Satb1* siRNA persistence and specificity and *Satb1* embryo staining.** A) Immunofluorescence of *Satb1* in 8-cell embryos (n=25). Embryo boundary is outlined in white. B) Quantification of immunofluorescence represented in A. Fluorescence quantified and normalized to the nucleus with the strongest staining per individual embryo. C) Immunofluorescence of *Satb1* in early blastocysts after being injected with control (n=14) or *Satb1* siRNA (n=18). D) Quantification of relative fluorescent intensity of *Satb1* staining from C. E) Confocal images of control and *Satb1* siRNA 1, *Satb1* siRNA 2 and *Satb1* siRNA 3 injected embryos. *Nanog*, (EPI), *Sox17* (PE) and *Cdx2* (TE) were used as lineage markers. Quantification of this experiment shown in F. F) Contribution of control (n=17) and *Satb1* siRNA 1 (n=19), 2 (n=21), and 3 (n=23) injected embryos to EPI, PE, and TE. G) qRT-PCR of control (n=47 embryos, three biological repeats), *Satb1* siRNA 1 (n=58 embryos, three biological repeats), *Satb1* siRNA 2 (n=53 embryos, three biological repeats), *Satb1* siRNA 3 (n=49 embryos, three biological repeats) injected embryos to investigate *Satb1* mRNA levels. Student's t-test was used to test significance \*= p<0.05, \*\*= p<0.01, \*\*\*= p<0.001. Error bars represent s.e.m. Scale bars, 10  $\mu$ m.



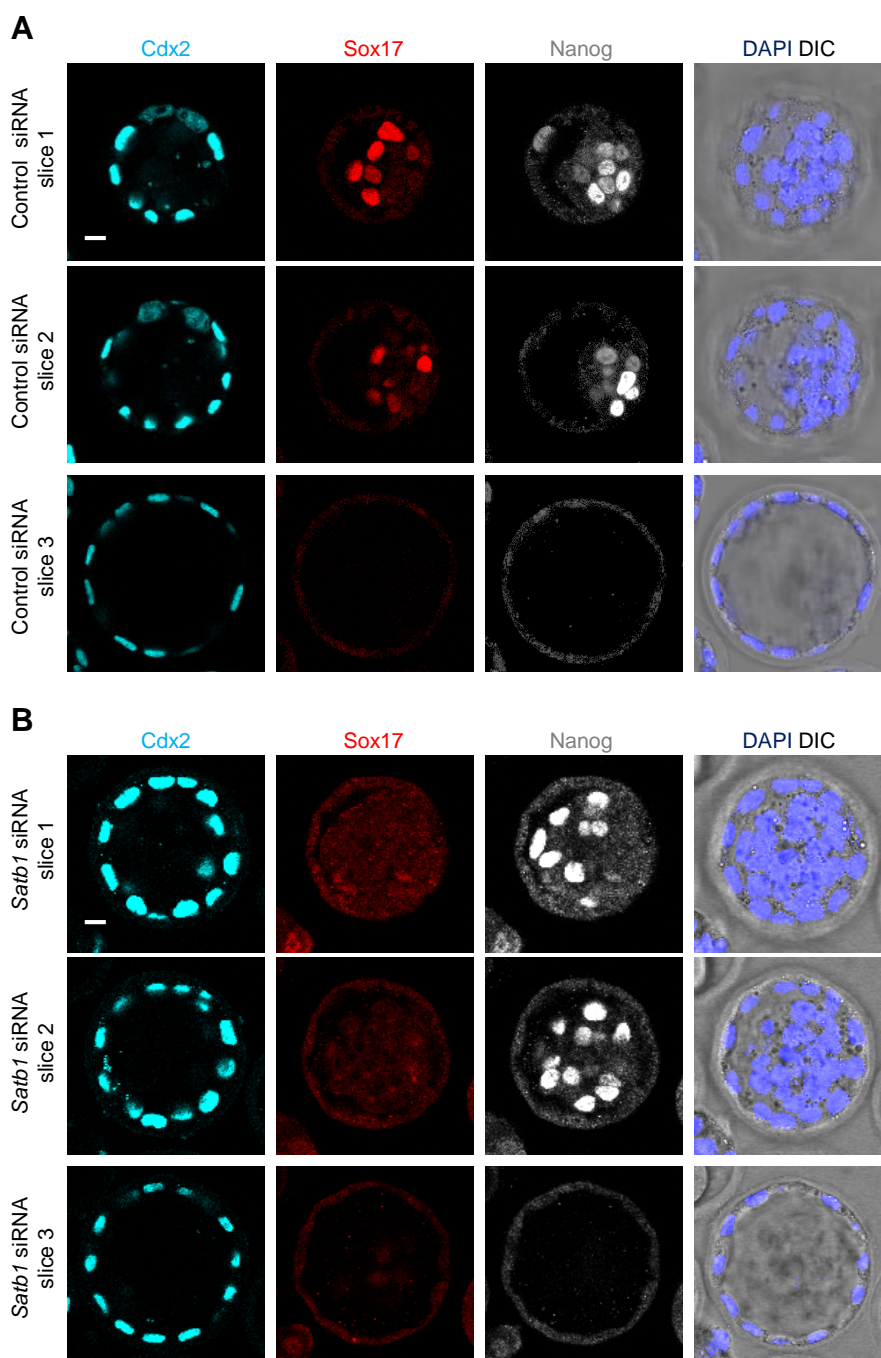


**Figure S2. Z-stack slices of confocal images from Figure 2E.** A) Slices of the confocal z-stack of the control siRNA injected embryo presented in Fig 2 E. Nanog, (EPI), Sox17 (PE) and Cdx2 (TE) were used as lineage markers B) Slices of the confocal Z-stack of the Satb1 siRNA injected embryo presented in Fig 2 E (Embryo 1). Nanog, (EPI), Sox17 (PE) and Cdx2 (TE) were used as lineage markers. Scale bars, 10  $\mu$ m.

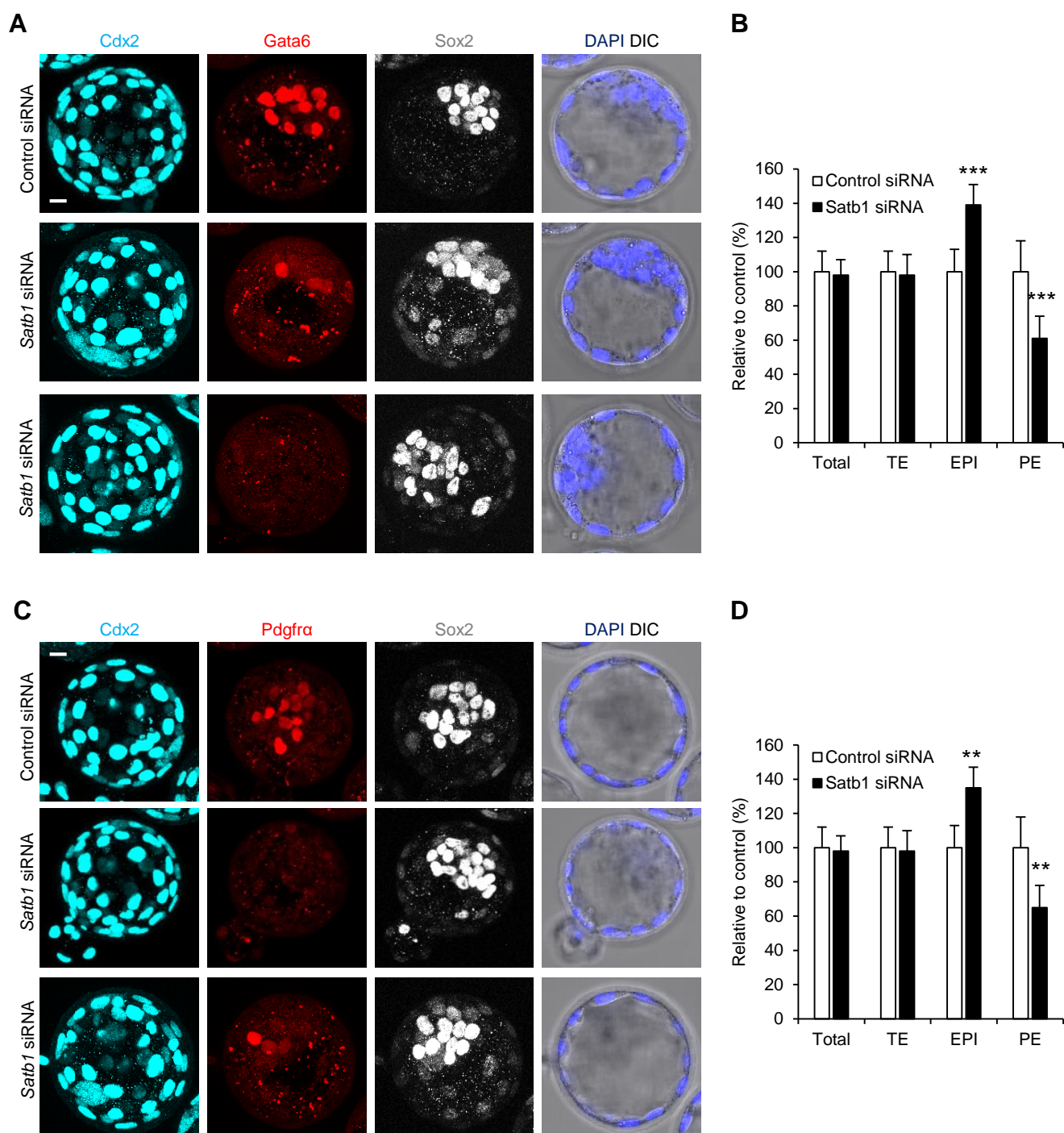


**Figure S3. *Satb1* siRNA phenotype assessed by Sox2, Gata6 and Pdgfra.** A) Confocal images of control (n=31) and *Satb1* siRNA (n=30) injected embryos. Sox2, (EPI), Gata6 (PE) and Cdx2 (TE) were used as lineage markers. B) Contribution of control and *Satb1* siRNA injected embryos represented in A to EPI, PE, and TE. C) Confocal images of control (n=27) and *Satb1* siRNA (n=29) injected embryos. Sox2, (EPI), Pdgfra (PE) and Cdx2 (TE) were used as lineage markers. D) Contribution of control and *Satb1* siRNA injected embryos represented in C to EPI, PE, and TE.

Student's t-test was used to test significance \*= p<0.05, \*\*= p<0.01. Error bars represent s.e.m. Scale bars, 10  $\mu$ m.

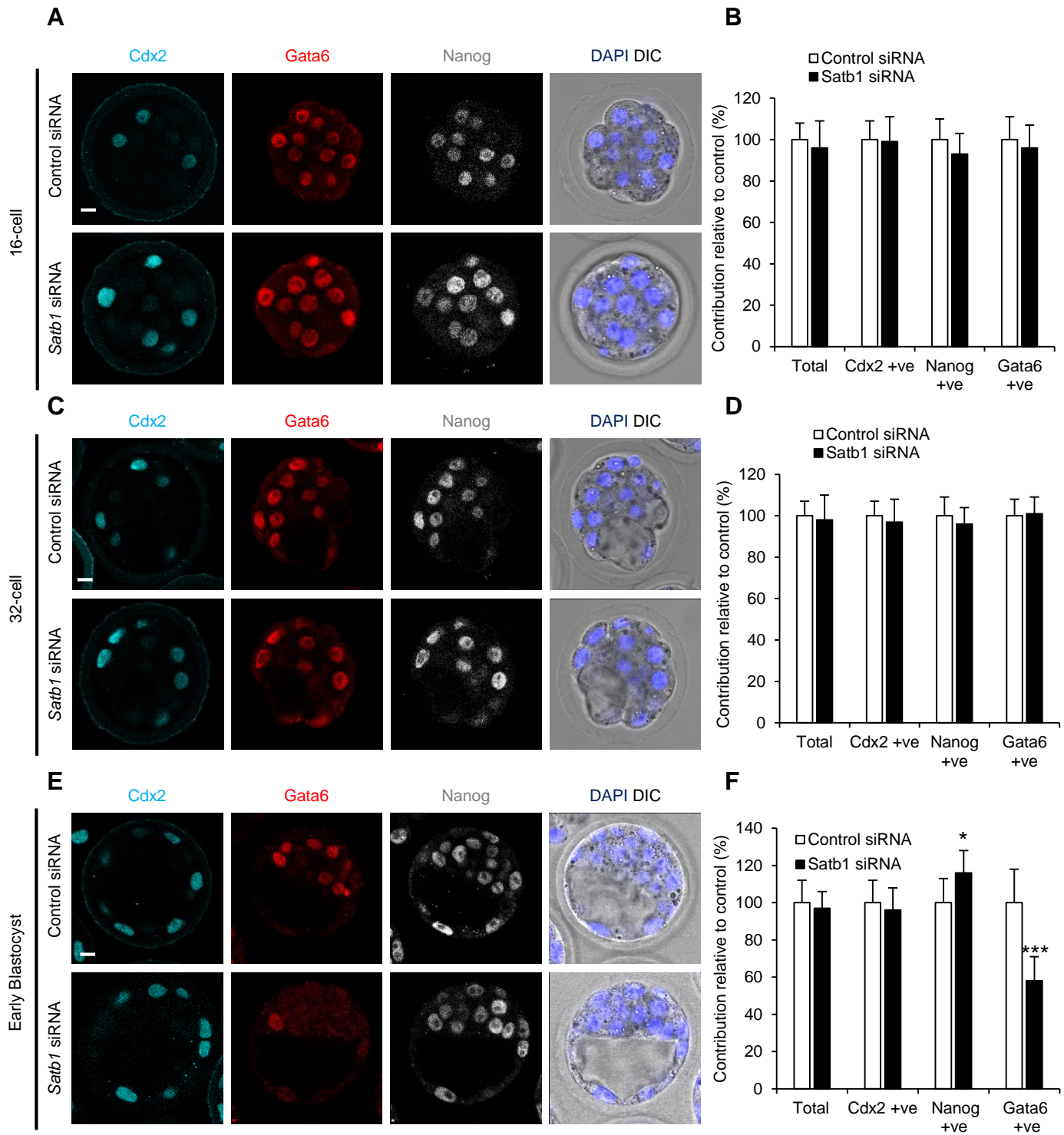


**Figure S4. Timing of effect of *Satb1* RNAi.** A) Confocal images of control (n=15) and *Satb1* siRNA (n=21) injected embryos at the 16-cell stage showing the localisation and distribution of Cdx2, Gata6 and Nanog. B) Relative number of blastomeres that are positive for Cdx2, Nanog and Gata6 from control and *Satb1* siRNA injected embryos represented in A. C) Confocal images of control (n=17) and *Satb1* siRNA (n=19) injected embryos at the 32-cell stage showing the localisation and distribution of Cdx2, Gata6 and Nanog. D) Relative number of blastomeres that are positive for Cdx2, Nanog and Gata6 from control and *Satb1* siRNA injected embryos represented in C. E) Confocal images of control (n=19) and *Satb1* siRNA (n=28) injected embryos at the early blastocyst stage showing the localisation and distribution of Cdx2, Gata6 and Nanog. F) Relative number of blastomeres that are positive for Cdx2, Nanog and Gata6 from control and *Satb1* siRNA injected embryos represented in E. Student's t-test was used to test significance \*=  $p < 0.005$ , \*\*\*=  $p < 0.001$ . Error bars represent s.e.m. Scale bars, 10  $\mu$ m.



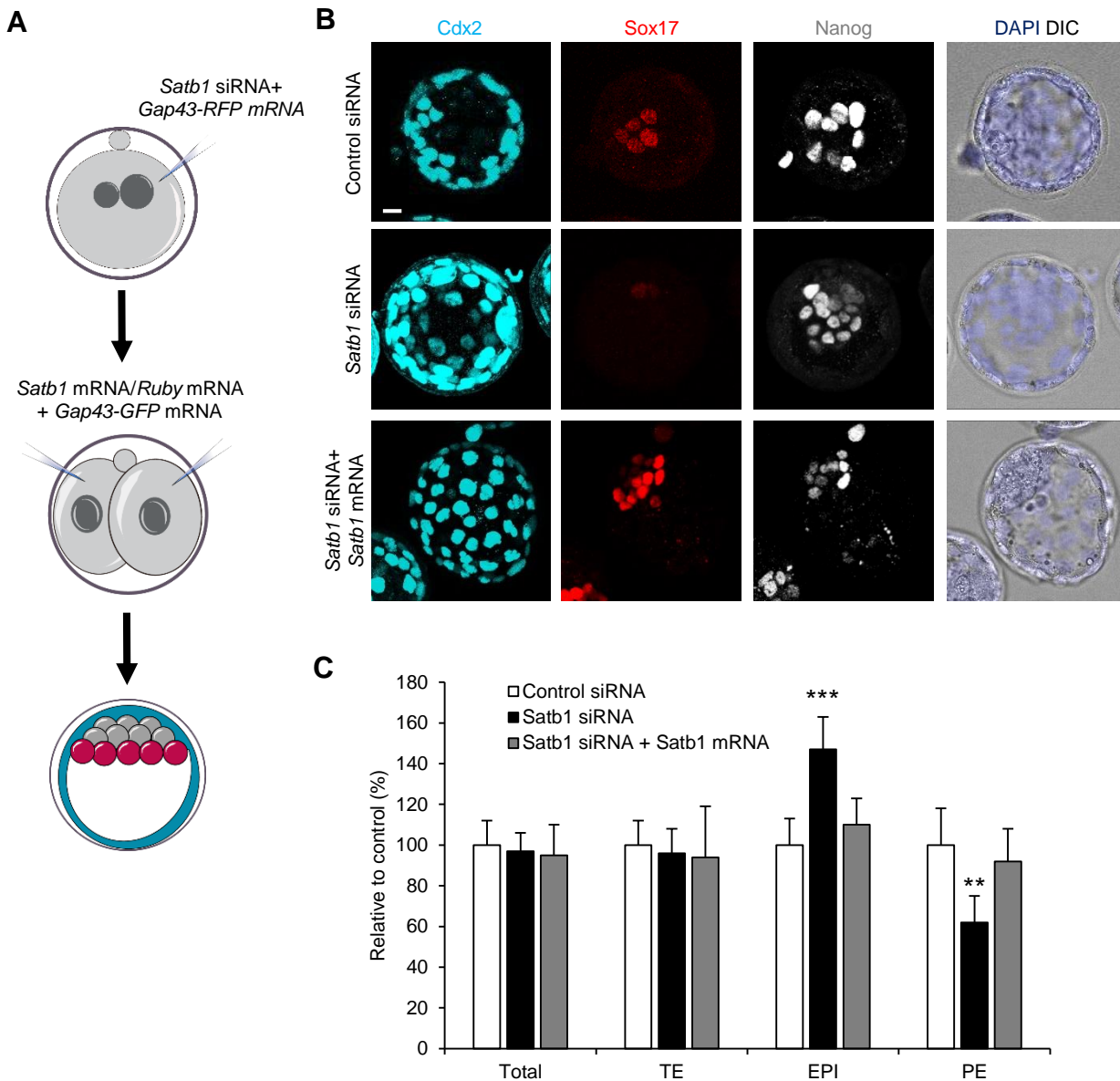


**Figure S5. Rescue of *Satb1* siRNA phenotype by *Satb1* mRNA.** A) Scheme of *Satb1* rescue experiment shown in B and C. Zygotes were injected with *Satb1* siRNA or control siRNA. At the 2-cell stage both blastomeres were then injected with either *Satb1* mRNA or *Ruby* mRNA as a control and then cultured until E4.5. B) Confocal images of control siRNA (n=12), *Satb1* siRNA (n=21) and *Satb1* siRNA + *Satb1* mRNA (n=26) injected embryos. Nanog (EPI), Sox17 (PE) and Cdx2 (TE) were used as lineage markers. C) Contribution of *Satb1* siRNA and *Satb1* siRNA + *Satb1* mRNA injected embryos to TE, PE and EPI, relative to control siRNA injected cells from experiment shown in B.

Student's t-test was used to test significance \*\*= p<0.01, \*\*\*= p<0.001. Error bars represent s.e.m. Scale bar, 10  $\mu$ m.

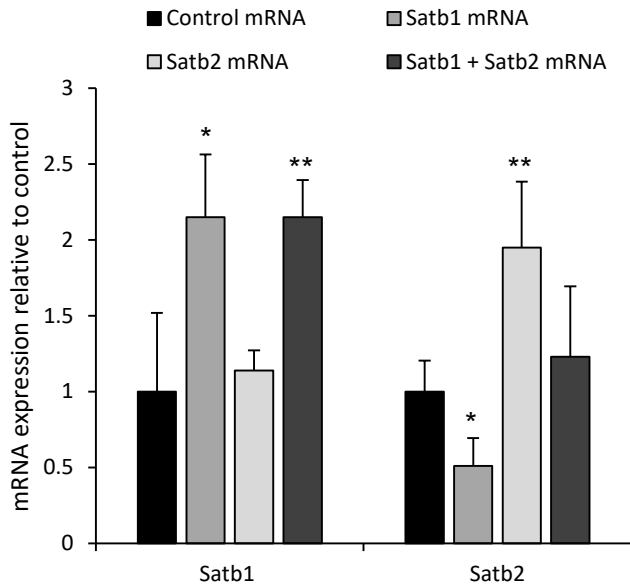


**Figure S6. Effect of Satb1 and Satb2 overexpression on Satb1 and Satb2 mRNA levels.** qRT-PCR of control (n=63 embryos, three biological repeats), Satb1 (n=71 embryos, three biological repeats), Satb2 (n=58 embryos, three biological repeats), Satb1 + Satb2 (n=47 embryos, three biological repeats) mRNA injected embryos to investigate Satb1 and Satb2 mRNA levels. Student's t-test was used to test significance \*\*=  $p < 0.01$ , \*\*\*=  $p < 0.001$ . Error bars represent s.e.m. Scale bar, 10  $\mu$ m.

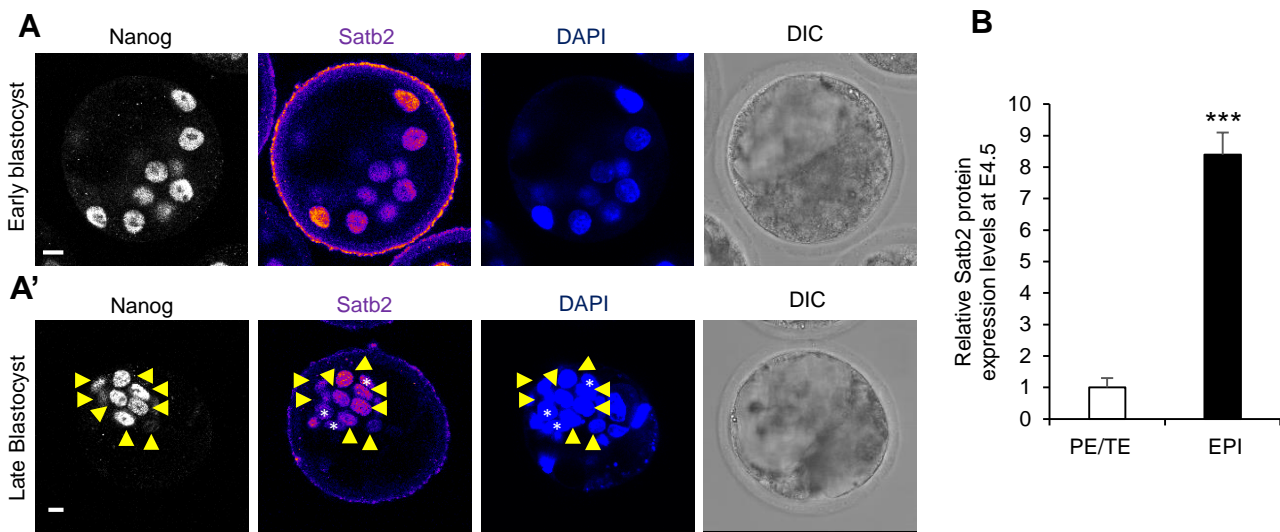


**Figure S7. Satb1 expression pattern in blastocysts.** A) Confocal images of Satb2 and Nanog staining in early blastocysts (n=12). A') Confocal images of Satb2 and Nanog staining in late blastocysts (n=16). Yellow arrows indicate EPI cells positive for Satb2 . White asterisks indicate PE cells positive for Satb2. B) Quantification of relative fluorescent intensity of Satb2 staining in EPI cells compared to PE/TE cells in late blastocysts as shown in A'. EPI cells were identified by the expression of Nanog. Scale bars, 10  $\mu$ m.